A GLOBALLY CONVERGENT CONVEXIFICATION ALGORITHM FOR THE INVERSE PROBLEM OF ELECTROMAGNETIC FREQUENCY SOUNDING IN ONE DIMENSION

M. V. Klibanov[1] **and A. Timonov**[1]

A globally convergent convexification algorithm for the numerical solution of the inverse problem of electromagnetic frequency sounding in one dimension is presented. This algorithm is based on the concept of convexification of a multiextremal objective function proposed recently by the authors. A key point in the proposed algorithm is that unlike conventional layer-stripping algorithms, it provides the stable approximate solution via minimization of a finite sequence of strictly convex objective functions resulted from applying the nonlinear weighted least squares method with Carleman's weight functions. The other advantage of the proposed algorithm is that its convergence to the "exact" solution does not depend on a starting vector. Thus, the uncertainty inherent to the local methods, such as the gradient or Newton-like methods, is eliminated. The 1-D inverse model of magnetotelluric sounding is selected to exemplify the convexification approach. Based on the localizing property of Carleman's weight functions, it is proven that the distance between the approximate and "exact" solutions is small if the approximation error is small. The results of computational experiments with several realistic and synthetic marine shallow water configurations are presented to demonstrate the computational feasibility of the proposed algorithm.

1. Introduction. In the recent paper [1] the authors have presented a new approach to inverse problems of frequency sounding called the convexification. The essence of convexification is constructing the strictly convex objective functions when applying the least squares method to the nonlinear coefficient inverse problems. It has been demonstrated in [1] that the conventional residual objective functions may often be multiextremal. Under such a condition, the gradient and Newton-like methods do not guarantee the convergence to a global minimum. Therefore, the numerical methods of global optimization, such as simulated annealing or genetic algorithms, are usually used to search for a global minimum. However, these methods are time-consuming even for several unknowns, and their use for solving the coefficient inverse problems has not been rigorously justified. The convexification approach can be considered as an alternative to the methods of global optimization. This paper is a more complete version of [19]. Compared to the latter, Sections 1 and 6 have been extended. Also, the complete proofs of Lemma 1 and Theorems 1 and 3 and Appendices A and B have been included.

In principle, the convexification approach is applicable to many inverse problems of frequency sounding of inhomogeneous media. For brevity, in this paper we focus on the inverse problem of magnetotelluric (MT) sounding of layered marine shallow water configurations (see Figure 1) and address rigorously the issue of multiextremality. Also, we demonstrate that the convexification approach can be applied to constructing a stable computational algorithm. The main advantage of the proposed algorithm is that it provides the convergence to the "exact" solution independent of the starting approximation. This is mainly because of the strict convexity of resulting objective functions.

Briefly, the convexification approach consists of the following stages. The original coefficient inverse problem is identically transformed to a certain auxiliary overdetermined boundary value problem for the nonlinear integro-differential equation that does not explicitly contain an unknown coefficient. The latter problem may also be interpreted in terms of continuation of the transformed field from the surface in an inhomogeneous layer. In the geophysics literature, such a procedure is referred to as the field prediction. The integro-differential operator is approximated by a family of parametric operators, where the parameter is chosen to be an upper bound of the frequency band. After that, the nonlinear weighted least squares method is applied to reduce the problem of field prediction to a constrained minimization problem. Once the transformed field in the inhomogeneous layer is found, the coefficient distribution is directly determined from this field. It should be emphasized that the use of Carleman's weight functions (CWF) is crucial for constructing the strictly convex objective functions. They result from Carleman estimates for the operator d^2/dz^2 (see Lemma 2 in Section 4).

[1] Department of Mathematics, University of North Carolina at Charlotte, Charlotte, NC 28223, USA; e-mail: mklibanv@email.uncc.edu; atimonov@email.uncc.edu

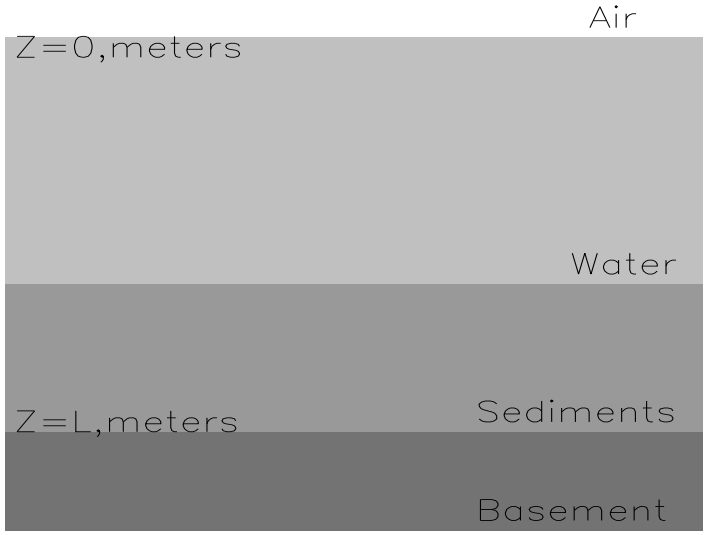

Figure 1: A typical marine shallow water configuration

Our choice of the specific model problem is motivated by the following. The principle of MT sounding was first formulated and investigated by Tikhonov [2, 3] and Cagniard [4] in the early fifties of the 20th century. Since then, the 1-D model of MT sounding has been extensively tested against a variety of simulated and field data for tectonic studies and geophysical exploration of mineral, oil and gas deposits (see, e.g., [5]). As a result, the consistency of this model with realistic horizontally-stratified (layered) media was demonstrated. Over the last two decades, the MT sounding methods have also been applied to marine induction studies in oceanography (see, e.g., [6, 7]). Since the marine configurations consist of the highly conductive seawater and porous sediments, the wave process is not practically established in such media. Therefore, the propagation of the electromagnetic (EM) field at sufficiently low frequencies is similar to the diffusion of light in highly absorbing media. It has been pointed out in the contemporary marine electromagnetics literature (see, e.g., [8]) that in shallow waters the EM signals can be accurately detected in the 1 Hz to 10 KHz frequency band. This frequency band is of particular interest to environmental science for underwater communication and navigation and detection and identification of objects submerged in the seawater or buried in the near-seafloor sediments. Although these applications require the use of controlled EM sources, such as electric or magnetic dipoles or line currents, it can be shown that the EM frequency sounding models are similar to the MT model. Therefore, one can take advantage of exploiting the more simple 1-D MT model in exemplifying the feasibility of convexification.

Since the eighties of the 20th century, the α-dependence of Tikhonov's smoothing functional has been extensively exploited in the Soviet (Russian) geophysics community (see, e.g., [11]) when applying various gradient and Newton-like methods to inverse problems of MT (EM) frequency sounding. Specifically, starting with sufficiently large value of α, the minimization problem for Tikhonov's smoothing functional is solved by either the gradient or Newton-like methods. The process is advancing in the direction of decrease of α until a certain stopping criterion is attained. In [12] such a technique for choosing the regularization parameter was formalized and referred to as the continuation method. In the contemporary mathematics literature (see, e.g., [9, 13]), this technique is referred to as outer-inner iterations (an outer iteration over α and an inner iteration with a gradient or Newton-like method). In [13], the outer-inner iteration scheme has been justified for one specific case when the original nonlinear operator can be decomposed into (or approximated by) a sum of linear and bilinear operators. However, the outer-inner iteration scheme requires many restarting procedures if there is no *a priori* information available about a certain approximation to the "exact" solution located in its small vicinity. The convexification approach can be considered as an alternative to the outer-inner iteration scheme in that it does not require multiple restarting procedures.

The MT (EM) sounding observations are usually available in the limited frequency band $[\tilde{\omega}_{\min}, \tilde{\omega}_{\max}]$ due

to both the physical and logistic reasons. In marine electromagnetics, the upper bound does not exceed a few hundred Hz. In other words, the sounding data are always incomplete. Furthermore, the application of the Tikhonov regularization scheme to a nonlinear inverse problem (see, e.g., [9, 10]) does not, in general, eliminate the multiextremality of Tikhonov's smoothing functional. Indeed, if the regularization parameter α is sufficiently large, the stabilizing term in Tikhonov's smoothing functional dominates over the residual one. Since the stabilizing term is quadratic, Tikhonov's functional may become even quasi-strictly convex. However, the minimizer of this functional may be sufficiently far from the "exact" solution. Conversely, if the regularization parameter is sufficiently small, the residual term dominates over the stabilizing one. So, the multiextremality of Tikhonov's smoothing functional may remain.

We address the issue of incompleteness of sounding data when constructing the sequential minimization algorithm based on the convexification approach. We certainly realize that *a priori* information about the problem has to be used when constructing the algorithm. In general, such information can be introduced in many ways. For instance, if the sediment characterization problem is our primary goal, the information about the conductivities of the air, seawater, basement, and the depth L of an inhomogeneous layer is usually available from the direct measurements or geological/geophysical survey. Such information can be used to construct the three layer support configuration containing the air, seawater and basement layers. It should be pointed out that such a support configuration is not necessarily close in a certain sense to a real configuration. Indeed, the conductivities and thicknesses of sediment layers may differ significantly (up to several times) from the conductivity of the seawater and the depth of water column. Solving analytically the forward problem for the support configuration, one can then simulate the data in a frequency band, which is broader than the actual frequency band available in sounding observations. Extending the actual frequency band, we substantially reduce the approximation errors when constructing the sequential minimization algorithm. It is proved in this paper that the smaller the approximation error the closer the approximate solution to the "exact" solution of the original inverse problem. Therefore, if a sufficiently broad frequency band is available in observations, there is no need for data extension.

Implementing the convexification approach to EM frequency sounding of layered conductive media, we exploit Theorem 5.1 from the paper [1]. However, we do not solve the corresponding minimization problem for the strictly convex objective function $J_{\lambda,\chi}(q)$ on a set $\mathcal{K}(m)$ as indicated in [1]. Instead, we construct its finite-dimensional analog as follows. We divide the interval $[0, L]$ into a finite set of subintervals and approximate the spatial dependence of the predicted field by a quadratic polynomial in each subinterval. The unknown coefficients of these polynomials are the frequency-dependent functions. Such an approximation is crucial for both the stability analysis and implementation of the algorithm. In the first subinterval, we use the given Dirichlet and Neumann conditions at $z = 0$ in order to obtain the coefficients at lower-order terms of the quadratic polynomial. Thus, only the leading coefficient of this polynomial is unknown. Applying the nonlinear weighted least squares method with Carleman's weight functions and taking into account the strict convexity and differentiability of the resulting objective function, we then formulate an inequality-constrained minimization problem with respect to this coefficient and solve it by the Generalized Reduced Gradient Method (GRGM) (see, e.g., [15]) avoiding the use of penalty functions. To ensure an appropriate accuracy, the constraints are obtained from the solution of the forward problem for the support configuration. The starting vector is directly computed from sounding data available from observations when determining the minimizer for the first subinterval. Once the leading coefficient is determined, the transformed field and its first derivative are computed at the right endpoint of the first subinterval. Then, they are used in the second subinterval to determine the starting vector. The algorithm is advancing into the inhomogeneous layer until the last subinterval is met.

The sequential minimization algorithm developed in this paper can be viewed as a new numerical technique allowing the stable field continuation into an inhomogeneous lossy layer. In the applied literature, this problem is referred to as the field prediction. The layer stripping approach has been recently developed to facilitate this problem. In the case of frequency sounding of a lossless inhomogeneous layer, the layer stripping approach has been rigorously justified (see, e.g., [16]) and some computational algorithms providing the stable solutions have been constructed (see, e.g., [17, 18]). However, it is very difficult to extend both these approach and algorithms to the case of a lossy inhomogeneous layer. The main reason is that the problem of determining the inverse Laplace transform connecting both cases is inherently unstable. Even being regularized, it does not allow sufficiently accurate solutions due to incompleteness of sounding data. To our knowledge, there are no layer stripping algorithms providing the stable solutions to the inverse problem of frequency sounding of lossy layered media. Unlike the layer stripping algorithms, the sequential minimization algorithm proposed in this paper is stable. The stabilization is due to Carleman's weight functions that suppress the exponential increase of error in the predicted field when advancing into an inhomogeneous layer.

The paper is arranged as follows. In Section 2, the 1-D forward and inverse models of MT shallow sounding are formulated. In Section 3, we introduce the concept of sequential minimization. In Section 4, we prove the strict convexity of objective functions resulted from applying the convexification approach. In Section 5, we present the stability analysis. Section 6 describes in detail the computational algorithm of sequential minimization and presents the numerical results. Finally, in Section 7, we make conclusions and discuss possible directions for the further work.

2. Formulations of problems

2.1. A forward model. In MT sounding, the natural sources of the electromagnetic field are used. These sources are mainly due to the solar activity in the ionosphere of the Earth and thunderstorms in its troposphere. Because of remote sources, the EM field varies very slowly in the horizontal directions on the Earth's surface allowing to assume that the EM field in layered media depends on depth. Therefore, we model the distant natural sources by a plane transversely-polarized wave normally incident on the surface. For brevity, we consider only the TE-mode of MT sounding assuming that $\mathbf{E} = (E_x, 0, 0)$ and $\mathbf{H} = (0, H_y, H_z)$, where $E_x(z, \tilde{\omega}) = E_0 \exp(i\tilde{\omega}t - k_a z)$ is the x-component of the electric field normally incident on the surface $z = 0$, $i = \sqrt{-1}$, $\tilde{\omega}$ is the angular frequency, and k_a is the wavenumber in the air. The TM-mode can be considered by analogy. Under these conditions, the Maxwell's and linear material equations can be reduced in an inhomogeneous layer $[0, L]$ to the scalar equation with respect to the normalized electric field $u(z, \tilde{\omega}) = E_x(z, \tilde{\omega})/E_x(0, \tilde{\omega})$

$$u''(z, \tilde{\omega}) - k^2(z, \tilde{\omega}) u(z, \tilde{\omega}) = 0, \quad 0 < z < L, \tag{1}$$

where $u'' = \partial^2 u/\partial z^2$, $k^2(z, \tilde{\omega}) = \tilde{\omega}^2 \varepsilon_0 \varepsilon \mu \big(1 + i \tan\delta(z, \tilde{\omega})\big)$ is the variable wavenumber, $\tan\delta(z, \tilde{\omega}) = \sigma(z)/\varepsilon_0 \varepsilon \tilde{\omega}$ is the loss tangent, and $\sigma(z)$ is the conductivity distribution. Here, the quantities $\varepsilon_0 = 8.85 \cdot 10^{-12}$ F/m, $\varepsilon > 0$, and $\mu = 4\pi \cdot 10^{-7}$ H/m are the absolute permittivity of vacuum, the relative permittivity, and the magnetic permeability of a medium. The magnetic permeability is assumed to be constant for all layers. Since $k(z, \tilde{\omega}) = \tilde{\omega}(n(z, \tilde{\omega}) + i\kappa(z, \tilde{\omega}))$ (where $n(z, \tilde{\omega}) = \sqrt{\frac{\varepsilon_0 \varepsilon \mu}{2}(\sqrt{1 + \tan^2\delta} + 1)}$ is the index of refraction characterizing the phase speed of an EM wave and $\kappa(z, \tilde{\omega}) = \sqrt{\frac{\varepsilon_0 \varepsilon \mu}{2}(\sqrt{1 + \tan^2\delta} - 1)}$ is the attenuation coefficient characterizing the speed of decay of an EM wave amplitude), in the highly conductive media ($\tan\delta \gg 1$), such as marine configurations, $n \approx \kappa = \sqrt{\mu\sigma(z)/\tilde{\omega}}$. This means that both the refraction and attenuation are mainly affected by the conductivity and the displacement currents are negligibly small at low frequencies. Therefore, we shall neglect the induction current density when considering conductive configurations. Such media cannot be considered in practice as waveguides because of their strong attenuating effect. Quite the reverse, the propagation of the EM field in such media is similar to the diffusion of light in absorbing media. In this paper, we restrict our attention to the conductive configurations only.

To derive the boundary conditions for Eq. (1), we exploit the continuity of tangential components of both the electric and magnetic fields at $z = 0$ and $z = L$. Since $H_y = (-i\tilde{\omega}\mu)^{-1} \partial E_x/\partial z$, we have two continuity conditions with respect to both E_x and $\partial E_x/\partial z$ at each interface. The surface admittance $Y(\tilde{\omega})$ is defined by

$$Y(\tilde{\omega}) = \frac{H_y(0, \tilde{\omega})}{E_x(0, \tilde{\omega})} = -\frac{1}{i\tilde{\omega}\mu} \frac{E_x'(0, \tilde{\omega})}{E_x(0, \tilde{\omega})} = -\frac{1}{i\tilde{\omega}\mu} u'(0, \tilde{\omega}). \tag{2}$$

The depth L is assumed to be known, and the half-space $z > L$ is filled with a homogeneous poorly conductive medium, which we refer to as a basement whose conductivity σ_b is known. Satisfying the continuity conditions at both the interfaces $z = 0$ and $z = L$, we obtain both the Dirichlet $u(0, \tilde{\omega}) = 1$ and Robin $u'(0, \tilde{\omega}) + i\tilde{\omega}\mu Y(\tilde{\omega}) u(0, \tilde{\omega}) = 0$ conditions at $z = 0$ and the Robin condition $u'(L, \tilde{\omega}) + k_b u(L, \tilde{\omega}) = 0$ at $z = L$. Here, $u' = \partial u/\partial z$ and $k_b(\tilde{\omega}) = \frac{\sqrt{2}}{2}(i + 1)\sqrt{\tilde{\omega}\mu\sigma_b}$. Note that since the transmission field in the half-space $z > L$ is proportional to $\exp(-k_b z)$, the radiation condition as $z \to \infty$ is satisfied. Adding the radiation condition as $z \to -\infty$, we arrive to the forward model that consists of two boundary value problems. The first problem

$$u''(z, \tilde{\omega}) - k_a^2(\tilde{\omega}) u(z, \tilde{\omega}) = 0, \quad z < 0, \tag{3}$$

$$u'(0, \tilde{\omega}) + i\tilde{\omega}\mu Y(\tilde{\omega}) u(0, \tilde{\omega}) = 0, \tag{4}$$

$$\lim_{z \to -\infty} \big(u(z, \tilde{\omega}) - \exp(-k_a z)\big) = 0 \tag{5}$$

governs the propagation of the EM field in the homogeneous half-space (the air) $z < 0$ with $k_a = \tilde{\omega}\sqrt{\varepsilon_a \varepsilon_0 \mu}$.

The second boundary value problem

$$u''(z,\tilde{\omega}) - i\mu\tilde{\omega}\sigma(z)u(z,\tilde{\omega}) = 0, \quad 0 < z < L, \tag{6}$$

$$u(0,\tilde{\omega}) = 1, \tag{7}$$

$$u'(L,\tilde{\omega}) + k_b(\tilde{\omega})u(L,\tilde{\omega}) = 0 \tag{8}$$

governs the propagation of the EM field in the inhomogeneous layer $0 < z < L$ containing the seawater and sediments. Since the admittance $Y(\tilde{\omega})$ can be determined from the electric and magnetic components of the electromagnetic field measured on the surface as indicated in (2), the boundary values problems (3) – (5) and (6) – (8) can be considered separately. Since the subject of our investigation is the inhomogeneous layer, we focus on the second problem.

Lemma 1. *For any bounded piecewise-continuous function* $\sigma(z) \geqslant \text{const} > 0$ *and for any* $\tilde{\omega} \in [\tilde{\omega}_{\min}, \infty)$ *the boundary value problem* (6) – (8) *has a unique solution* $u \in H^2(0,L)$ *and* $u(z,\tilde{\omega}) \neq 0$ *for all* $(z,\tilde{\omega}) \in [0,L] \times [\tilde{\omega}_{\min}, \infty)$.

The proof of this lemma is indicated in Appendix A.

For computational reasons, we introduce the dimensionless variables $\xi = z/L$ and $\omega = \tilde{\omega}/\tilde{\omega}_{\min}$. Then, problem (6) – (8) can be rewritten in dimensionless form as follows:

$$u''(\xi,\omega) - \hat{k}^2(\xi,\omega)u(\xi,\omega) = 0, \quad 0 < \xi < 1, \tag{9}$$

$$u(0,\omega) = 1, \tag{10}$$

$$u(1,\omega) + \hat{k}_b(\omega)u(1,\omega) = 0, \tag{11}$$

where $\hat{k}^2(\xi,\omega) = iL^2\tilde{\omega}_{\min}\omega\mu\sigma(\xi)$ and $\hat{k}_b(\omega) = \frac{\sqrt{2}}{2}(i+1)L\sqrt{\tilde{\omega}_{\min}\omega\mu\sigma_b}$.

2.2. An inverse model. In practice, the horizontal components E_x and H_y of the electromagnetic field are measured on the surface $\xi = 0$. The admittance $Y(\omega)$ and, hence, the vertical gradient $u'(0,\omega) = -i\omega\mu Y(\omega)$ can also be determined from (2). The inverse problem of 1-D MT frequency sounding can then be formulated as follows.

Inverse Problem I. *Given the function* $u'(0,\omega) = \varphi(\omega)$, $\omega \in [1,\infty)$, *the normalized electric field satisfies the equations* (9) – (11). *Find the conductivity profile* $\sigma(\xi)$, $\xi \in (0,1)$.

In practice, the frequency dependence of both components of the electromagnetic field are always measured in the limited frequency band $[1,\omega_{\max}]$. Under these conditions, the formulation given by Inverse Problem I is not consistent with the reality. Therefore, we formulate the following problem.

Inverse Problem II. *Given the function* $u'(0,\omega) = \varphi(\omega)$, $\omega \in [1,\omega_{\max}]$, *the normalized electric field satisfies the equations* (9) – (11). *Find a certain approximation* $\tilde{\sigma}(\xi)$ *of the conductivity profile* $\sigma(\xi)$.

We shall make this formulation more specific in Section 3.2. It should also be pointed out that this formulation follows directly from Tikhonov's model of 1-D MT sounding [2, 3]. It was showed in [20] that Tikhonov's model can be reduced to the Sturm–Liouville equation via the Laplace-like transform. This gives rise to an alternative approach to the 1-D MT problem based on the Gelfand–Levitan equation (see the overview in [21]). Some algorithms for the inverse Sturm–Liouville problem and their numerical implementations can be found in [22, 23]. It should, however, be noted that in the case of incomplete sounding data, the accuracy of the reconstructed potential may severely be affected by the inverse Laplace-like transform. In the convexification approach, we use Tikhonov's model of MT sounding.

3. The general scheme of sequential minimization. In the paper [1], it was shown that Inverse Problem II can be reduced to the problem of minimization of the strictly convex functional $J_{\lambda,\chi}(p)$ on the compact set $\mathcal{K}(M)$. In this paper, our primary goal is to construct a stable computational algorithm for solving this problem. To achieve this goal, we introduce the concept of sequential minimization. Specifically, instead of minimizing the functional $J_{\lambda,\chi}(p)$ on the compact set $\mathcal{K}(M)$, we formulate a finite sequence of more simple minimization problems and solve them recursively starting from the surface $\xi = 0$ and advancing in the inhomogeneous layer. We apply this concept to the 1-D inverse problem of frequency sounding in the four stages: (1) transformations of the original inverse problem to an auxiliary boundary value problem for an integro-differential equation; (2) approximation of the integro-differential operator; (3) the sequential minimization; (4) inversion of sounding data.

3.1. Transformations In just the same way as we did before (see [1], Section 4), we introduce the function

$w(\xi,\omega)=\ln[u(\xi,\omega)]/\omega$ and transform the problem (9)–(11) to the following problem:

$$w''+\omega(w')^2=i\mu L^2\tilde{\omega}_{\min}\sigma(\xi),\quad 0<\xi<1, \tag{12}$$

$$w(0,\omega)=0, \tag{13}$$

$$w'(0,\omega)=\varphi(\omega)/\omega, \tag{14}$$

$$w'(1,\omega)=-\hat{k}_b/\omega, \tag{15}$$

where $\varphi(\omega)=u'(0,\omega)$. Next, introducing the function

$$p(\xi,\omega)=\frac{\partial}{\partial\omega}\left[w(\xi,\omega)-\xi\,\frac{\varphi(\omega)}{\omega}\right] \tag{16}$$

and using the definition of antiderivative, i.e., $w(\xi,\omega)-\xi\frac{\varphi(\omega)}{\omega}=-\int_\omega^\infty p(\xi,\nu)\,d\nu$, we obtain the boundary value problem for the integro-differential equation:

$$p''-2\omega p'\int_\omega^\infty p'(\xi,\nu)d\nu+\left(\int_\omega^\infty p'(\xi,\nu)\,d\nu\right)^2$$
$$-2\,\frac{d\varphi(\omega)}{d\omega}\int_\omega^\infty p'(\xi,\nu)\,d\nu+2\varphi(\omega)p'-F(\omega)=0,\quad 0<\xi<1, \tag{17}$$

$$p(0,\omega)=0,\quad p'(0,\omega)=0, \tag{18}$$

$$p'(1,\omega)=\Psi(\omega), \tag{19}$$

where

$$F(\omega)=\frac{\varphi(\omega)}{\omega}\left[\frac{\varphi(\omega)}{\omega}-2\frac{d\varphi(\omega)}{d\omega}\right], \tag{20}$$

$$\Psi(\omega)=\frac{1}{\omega}\left[\frac{\hat{k}_b(\omega)+\varphi(\omega)}{\omega}-\frac{d\hat{k}_b(\omega)}{d\omega}-\frac{d\varphi(\omega)}{d\omega}\right]. \tag{21}$$

We note that the convergence of the integral term in (17) was proven in [1] for the 3-D case. A similar result for the 1-D case is presented in Appendix B. Thus, Inverse Problem II is reduced to the overdetermined problem (17)–(21) with respect to the function $p(\xi,\omega)$. One can notice that the latter problem does not contain explicitly the coefficient $\sigma(\xi)$. Instead, it includes the functions $F(\omega)$ and $\Psi(\omega)$ that are determined via the sounding data $\varphi(\omega)$. Since these formal transformations simply scale the normalized field $u(\xi,\omega)$, we observe that the coefficient inverse problem is reduced to the problem of continuation of the scaled electric field from the surface $\xi=0$ into the inhomogeneous layer. In the applied literature (see, e.g., [8]), such a problem is referred as to the field prediction. Once the field prediction problem is solved, the first and second spatial derivatives of $w(\xi,\omega)$ are computed from the predicted field and, hence, the conductivity distribution is determined from Eq. (12).

3.2. Approximations. We first approximate the operator generated by the auxiliary problem (17)–(21) as follows. Representing the integral of p' as

$$\int_\omega^\infty p'(\xi,\nu)\,d\nu=\int_\omega^\Omega p'(\xi,\nu)\,d\nu+\int_\Omega^\infty p'(\xi,\nu)\,d\nu, \tag{22}$$

we rewrite the problem (17)–(19) in the form

$$L_\Omega(p)-F(\omega)=F_r(\xi,\omega;\Omega),\quad 0<\xi<1, \tag{23}$$

$$p(0,\omega)=0,\quad p'(0,\omega)=0, \tag{24}$$

$$p'(1,\omega)=\Psi(\omega), \tag{25}$$

where

$$L_\Omega(p)\equiv p''-2\omega p'\cdot\int_\omega^\Omega p'(\xi,\nu)\,d\nu+\left(\int_\omega^\Omega p'(\xi,\nu)\,d\nu\right)^2-2\,\frac{d\varphi(\omega)}{d\omega}\cdot\int_\omega^\Omega p'(\xi,\nu)\,d\nu+2\varphi(\omega)p' \tag{26}$$

and

$$F_r(\xi,\omega;\Omega)=\int_\Omega^\infty p'(\xi,\nu)\,d\nu\cdot\left[2\omega p'+2\,\frac{d\varphi(\omega)}{d\omega}-2\int_\omega^\Omega p'(\xi,\nu)\,d\nu-\int_\Omega^\infty p'(\xi,\nu)\,d\nu\right]. \tag{27}$$

Let $(a,b) \subseteq (0,1)$ be an arbitrary interval and $s \geqslant 0$ be an integer number. We define the space

$$C^s_\Omega[a,b] = \left\{ f(\xi,\omega) : f \in C([a,b]\times[1,\Omega]),\ \|f\|_{C^s_\Omega[a,b]} = \max_{j\in[0,s]} \max_{(\xi,\omega)} \left| \frac{\partial^j}{\partial \xi^j} f(\xi,\omega) \right| < \infty \right\}.$$

Since the frequency Ω is chosen so that the magnitude of the second term in the right-hand side of (22) is sufficiently small, it is meaningful to assume that there exists a sufficiently small number $\tilde{\varepsilon} > 0$ such that

$$\|F_r\|_{C_\Omega[0,1]} < \tilde{\varepsilon}. \tag{28}$$

Therefore, we approximate the problem (17) – (19) by neglecting the term $F_r(\xi,\omega;\Omega)$. The approximating boundary value problems have the form

$$L_\Omega(p) - F(\omega) = 0, \quad 0 < \xi < 1, \quad \omega \in [1,\Omega], \tag{29}$$

$$p(0,\omega) = 0, \quad p'(0,\omega) = 0, \tag{30}$$

$$p'(1,\omega) = \Psi(\omega), \tag{31}$$

It should be emphasized that the smallness of the integral $\int_\Omega^\infty p'(\xi,\nu)\,d\nu$ requires the proper choice of the "cutting" frequency Ω. It would certainly be desirable to take $\Omega = \omega_{\max}$. However, this is possible only if a sufficiently large upper bound $\omega_{\max}$ of the frequency band is available in MT (EM) sounding. Otherwise, the sounding data need to be extended to the interval $(\omega_{\max},\Omega]$ prior to applying the sequential minimization algorithm. Such an extension provides an appropriately small approximation error and, hence, a small error in the recovered conductivity. If this is the case, we face with the problem of analytic continuation. Indeed, let the domain of the analytic function $\varphi(\omega)$ be $[1,\infty)$. However, this function is determined only on the interval $[1,\omega_{\max}]$. We wish to find the function $\varphi(\omega)$ in $(\omega_{\max},\Omega]$, $\Omega > \omega_{\max}$. It is well known that the problem of analytic continuation is, in general, unstable. Although the continuous dependence of the recovered conductivity distribution on perturbations of data is proven in Section 5, we should take special care when constructing a regularized analytic continuation. The main criterion is to minimize the error of analytic continuation as much as possible. This can be done in several ways. Although a detailed discussion of this problem is out of the scope of this paper, we indicate in Section 6 a specific procedure for extending the sounding data when dealing with marine configurations. This procedure exploits the support configuration allowing for reducing the approximation error.

Let u^* be the solution of the forward problem (9) – (11) corresponding to an "exact" conductivity profile σ^* such that $\varphi^*(\omega) = u^{*\prime}(0,\omega)$. Since all transformations indicated in Section 3.1 are identical, the function

$$p^*(\xi,\omega) = \frac{\partial}{\partial\omega}\left[\frac{\ln u^* - \xi\varphi^*}{\omega}\right]$$

satisfies the conditions (23) – (25). We formulate the problem of finding a certain approximation of the function p^* as follows.

Given $\tilde{\varepsilon}$ and approximate data $\tilde{\varphi}$ such that $\tilde{\varphi} = \varphi^* + \Delta\varphi$, $\omega \in [1,\Omega]$, $\|\Delta\varphi\|_{C^1[1,\Omega]} \leqslant \delta$, $\delta > 0$ (where $\delta > 0$ and $\tilde{\varepsilon}$ are sufficiently small constants), find a certain function $\tilde{p}(\xi,\omega)$ close to the function $p^*(\xi,\omega)$, $\{(\xi,\omega) : (\xi,\omega) \in [0,1]\times[1,\Omega]\}$.

To solve this problem numerically, we construct a least squares solution to the overdetermined problem (29) – (31) as follows. For each fixed $\omega \in [1,\Omega]$, we first divide the interval $[0,1]$ into $(n-1)$ subintervals

$$0 = \xi_0 < \xi_1 < \xi_2 < \ldots < \xi_{n-2} < \xi_{n-1} = 1.$$

For brevity, we consider below only a uniform grid. Then we approximate the function $p(\xi,\omega)$ in each subinterval $[\xi_{i-1},\xi_i]$ $(i = 1,2,\ldots,n-1)$ by a quadratic polynomial. The step size $h = 1/(n-1)$ is chosen to be sufficiently small in order to ensure a small error of approximation of the function $p(\xi,\omega)$ by a second degree polynomial. Because of zero Dirichlet and Neumann conditions at $\xi = 0$, we construct the approximation

$$p(\xi,\omega) \approx p_1(\xi,\omega) = \frac{1}{2}\,a_1(\omega)\xi^2, \quad \xi \in (0,\xi_1]. \tag{32}$$

Assuming that the function $p_{i-1}(\xi,\omega)$ is known, we derive the recurrence formulas for approximations of $p(\xi,\omega)$ on the subintervals $(\xi_{i-1},\xi_i]$ $(i = 2,3,\ldots,n-2)$:

$$p(\xi,\omega) \approx p_i(\xi,\omega) = \frac{1}{2}\,a_i(\omega)(\xi-\xi_{i-1})^2 + p'_{i-1}(\xi_{i-1},\omega)(\xi-\xi_{i-1}) + p_{i-1}(\xi_{i-1},\omega), \quad \xi \in (\xi_{i-1},\xi_i]. \tag{33}$$

Taking into account the Neumann condition at $\xi = 1$, we obtain the following approximation on $(\xi_{n-2}, \xi_{n-1}]$:

$$p(\xi,\omega) \approx p_{n-1}(\xi,\omega) = \frac{1}{2}\,a_{n-1}(\omega)(\xi-\xi_{n-2})\cdot\left[(\xi-\xi_{n-2}) - \frac{2}{n}\right] + \Psi(\omega)(\xi-\xi_{n-2}) + p_{n-2}(\xi_{n-2},\omega), \quad \xi \in (\xi_{n-2},\xi_{n-1}]. \tag{34}$$

Thus, the function $p(\xi,\omega)$ is approximately determined by the $(n-1)$ unknown coefficients a_i $(i = 1, 2, \ldots, n-1)$. This allows us to reduce the nonlinear least squares problem (5.9) from [1] to a sequence of more simple minimization problems with respect to each a_i.

3.3. Sequential minimization

3.3.1. Constructing the objective functions. Let $M > 0$ be a certain constant. In the space $C^2_\Omega[0,1]$ we consider a convex compact set

$$G(M) = \left\{ g(\xi,\omega) : g \in C^3_\Omega[0,1] : \|g\|_{C^3_\Omega[0,1]} \leqslant M,\ M > 0 \right\}.$$

In the space $C[1,\Omega]$ we also consider a convex bounded set

$$\tilde{G}(M) = \left\{ q(\omega) : q \in C[1,\Omega] : \|q\|_{C[1,\Omega]} \leqslant M \right\}.$$

By analogy with [1], we consider Carleman's weight functions (CWFs)

$$C_{\lambda,i}(\xi) = \exp\left[-\frac{\lambda}{2}(\xi-\xi_{i-1})\right], \quad \xi \in [\xi_{i-1},\xi_i), \tag{35}$$

where $\lambda > 0$ is a sufficiently large parameter, and a sequence of functionals

$$J_{\lambda,i}(a_i) = \int_1^\Omega \int_{\xi_{i-1}}^{\xi_i} \left|\hat{L}_\Omega(a_i) - F(\omega)\right|^2 C^2_{\lambda,i}(\xi)\,d\xi\,d\omega, \tag{36}$$

where $\hat{L}_\Omega(a_i)$ is the value of the integro-differential operator $L_\Omega(p)$ on the subintervals $[\xi_{i-1},\xi_i]$ at the function $p(\xi,\omega)$ defined by (33) and (34).

Since both the functions $p(\xi_{i-1},\omega)$ and $p'(\xi_{i-1},\omega)$ are known from the preceding iteration, the only function $a_i(\omega)$ is unknown on $[\xi_{i-1},\xi_i]$.

3.3.2. The procedure of sequential minimization. Consider the finite sequence of constrained minimization problems

$$\operatorname{argmin}\left\{ J_{\lambda,i}(a_i) : a_i(\omega) \in \tilde{G}(M), (i = 1, 2, ..., n-1) \right\}, \tag{37}$$

where

$$J_{\lambda,i}(a_i) = \int_1^\Omega \int_{\xi_{i-1}}^{\xi_i} \left|\hat{L}_\Omega(a_i) - F(\omega)\right|^2 C^2_{\lambda,i}(\xi)\,d\xi\,d\omega. \tag{38}$$

These problems (37) can only be recursively solved. Introducing the functions $\rho_i(\xi), \eta_i(\xi,\omega)$

$$\rho_i(\xi) = \begin{cases} \xi, & \xi \in [\xi_0,\xi_1], \\ \xi - \xi_{i-1}, & \xi \in (\xi_{i-1},\xi_i] \quad (i = 2,\ldots,n-2), \\ (\xi-\xi_{n-2}) - 1/n, & \xi \in (\xi_{n-2},\xi_{n-1}], \end{cases} \tag{39}$$

$$\eta_i(\xi,\omega) = \begin{cases} 0, & \xi \in [\xi_0,\xi_1], \\ p'_{i-1}(\xi_{i-1},\omega), & \xi \in (\xi_{i-1},\xi_i] \quad (i = 2,\ldots,n-2), \\ \Psi(\omega), & \xi \in (\xi_{n-2},\xi_{n-1}], \end{cases} \tag{40}$$

we obtain

$$\begin{aligned} \hat{L}_\Omega(a_i) = a_i &- 2\omega(a_i\rho_i^2 + \eta_i)\int_\omega^\Omega a_i(\nu)\,d\nu - 2\omega(a_i\rho_i^2+\eta_i)\int_\omega^\Omega \eta_i(\xi,\nu)\,d\nu \\ &+ \rho_i^2\left(\int_\omega^\Omega a_i(\nu)\,d\nu\right)^2 + \left(\int_\omega^\Omega \eta_i(\xi,\nu)\,d\nu\right)^2 + 2\rho_i\int_\omega^\Omega a_i(\nu)\,d\nu\int_\omega^\Omega \eta_i(\xi,\nu)\,d\nu \\ &- 2\,\frac{d\varphi}{d\omega}\,\rho_i\int_\omega^\Omega a_i(\nu)\,d\nu - 2\,\frac{d\varphi}{d\omega}\int_\omega^\Omega \eta_i(\xi,\nu)\,d\nu + 2\varphi\rho_i a_i + 2\varphi\eta_i. \end{aligned} \tag{41}$$

Since the functions $\eta_i(\xi,\omega)$ are recursively computed, the operators $\hat{L}_\Omega(a_i)$ and functionals $J_{\lambda i}(a_i)$ are also recursively found. This feature motivates the term "the sequential minimization". Specifically, we first solve numerically the constrained minimization problem (37) for $i=1$ computing the approximate minimizer $\tilde{a}_1$. We then use the expression (32) to calculate the approximations of $p_1(\xi_1,\omega)$ and $p_1'(\xi_1,\omega)$ and, hence, to compute $\hat{L}_\Omega(a_2)$, $J_{\lambda,i}(a_2)$ and the minimizer $\tilde{a}_2$, etc. until the last minimizer $\tilde{a}_{n-1}$ becomes computed. Note that the expressions (33) and (34) are used to calculate the approximations of $p_i'(\xi_i,\omega)$ for $i=2,\ldots,n-1$. For the existence and uniqueness of minimizers $\tilde{a}_i$, see Lemma 5.

3.4. Inversion. Once the minimizers $\tilde{a}_i(\omega)$ are found, the approximate first and second derivatives of the predicted field $\tilde{p}(\xi,\omega)$ are determined as

$$\tilde{p}'(\xi,\omega)=\begin{cases}\tilde{a}_1(\omega)\xi, & \xi\in[\xi_0,\xi_1],\\ \tilde{a}_i(\omega)(\xi-\xi_{i-1})+\tilde{p}'_{i-1}, & \xi\in(\xi_{i-1},\xi_i]\quad(i=2,\ldots,n-2),\\ \tilde{a}_{n-1}(\omega)\big[(\xi-\xi_{n-2})-1/n\big]+\Psi(\omega), & \xi\in(\xi_{n-2},\xi_{n-1}],\end{cases}\tag{42}$$

$$\tilde{p}''(\xi,\omega)=\begin{cases}\tilde{a}_1(\omega), & \xi\in[\xi_0,\xi_1],\\ \tilde{a}_i(\omega), & \xi\in(\xi_{i-1},\xi_i]\quad(i=2,\ldots,n-1).\end{cases}\tag{43}$$

These approximate derivatives can be used to determine the approximate conductivity. Indeed, it has been indicated in Section 3.1 that

$$\begin{aligned}w(\xi,\omega)&=-\int_\omega^\infty p(\xi,\nu)\,d\nu+\xi\,\frac{\varphi(\omega)}{\omega}=-\int_\omega^\Omega p(\xi,\nu)\,d\nu-\int_\Omega^\infty p(\xi,\nu)\,d\nu+\xi\,\frac{\varphi(\omega)}{\omega}\\&=-\int_\omega^\Omega p(\xi,\nu)\,d\nu+w(\xi,\Omega)+\xi\,\frac{\varphi(\omega)}{\omega}.\end{aligned}$$

If the frequency Ω is sufficiently large, the functions $w(\xi,\Omega)$, $w'(\xi,\Omega)$, and $w''(\xi,\Omega)$ are small. Therefore, we may approximate the functions w' and w'' by

$$\tilde{w}'(\xi,\omega)=-\int_\omega^\Omega \tilde{p}'(\xi,\nu)\,d\nu+\frac{\varphi(\omega)}{\omega}+w_s'(\xi,\Omega),\tag{44}$$

$$\tilde{w}''(\xi,\omega)=-\int_\omega^\Omega \tilde{p}''(\xi,\nu)\,d\nu+w_s''(\xi,\Omega),\tag{45}$$

where $w_s(\xi,\Omega)$ is the w-field at the frequency Ω for the support configuration (see Section 6.1), which is known. Since the right-hand side of Eq. (12) does not depend on ω, its left-hand side, i.e., the expression $w''+\omega(w')^2$, does not depend on ω as well. In principle, one can choose a certain fixed frequency $\omega\in[1,\Omega)$ in (44) – (45) when solving Eq. (12) with respect to $\sigma(\xi)$. To reduce the approximation error, we however choose $\omega=1$. Then we obtain the explicit formula for the solution of Inverse Problem II:

$$\tilde{\sigma}(\xi)=\frac{1}{\mu L^2\tilde{\omega}_{\min}}\big[2\alpha_i\Re(I_i)\Im(I_i)+\Re(\beta_i)\Im(I_i)+\Re(I_i)\Im(\beta_i)+\Im(\gamma_i)\big],\tag{46}$$

where $I_i=-\int_1^\Omega a_i(\nu)\,d\nu$, $\alpha_i=\omega\rho_i^2(\xi)$, $\beta_i=1+2\omega\tau_i(\xi)\rho_i(\xi)$, $\gamma_i=\omega\tau_i^2(\xi)$, and

$$\tau_i(\xi)=\begin{cases}\varphi(1), & \xi\in[\xi_0,\xi_1],\\ \varphi(1)+\int_1^\Omega p'_{i-1}\,d\nu, & \xi\in(\xi_{i-1},\xi_i]\quad(i=2,\ldots,n-2),\\ \varphi(1)+\int_1^\Omega \Psi d\nu, & \xi\in(\xi_{n-2},\xi_{n-1}].\end{cases}\tag{47}$$

4. Convexity analysis. Before establishing the strict convexity of functionals $J_{\lambda,i}$, we prove two lemmas. We show first that the CFWs (35) provide a Carleman-like estimate for the operator $d^2/d\xi^2$.

Remark 4.1. Actually, we extend the conventional definition of a strictly convex functional in a finite-dimensional space. The inequality (60) in Theorem 1 can be viewed as such an extended definition. In the finite-dimensional case, it turns out to be the conventional definition of the strict convexity because of equivalence of all norms under consideration.

Lemma 2. *For any complex-valued function $u \in H^2(0,l)$, $l = \text{const} > 0$, such that $u(0) = u'(0) = 0$, and for any number $\lambda > 0$ the following Carleman-like estimate holds:*

$$\int_0^l |u''|^2 \exp(-2\lambda x)\, dx \geqslant 2\lambda^3 (1+l)^{-2} \int_0^l |u|^2 \exp(-2\lambda x)\, dx. \tag{48}$$

Remark 4.2. Unlike the conventional Carleman estimates for the n-dimensional Laplace operator (see, e.g., [24, 25, 27]), the estimate (48) does not require a zero condition at the right endpoint $z = l$. On the other hand, we do not use the term

$$\lambda \int_0^l |u'|^2 \exp(-2\lambda x)\, dx$$

in the right-hand side of the inequality (48). This term can though be introduced under the assumptions that $u(l) = 0$ and the parameter λ is sufficiently large.

Remark 4.3. By virtue of (48), the $L_2(0,l)$-weighted norm of the second derivative $u''(x)$ dominates over the same norm of the function $u(x)$ for a sufficiently large λ. This fact is exploited to prove the results indicated below.

Proof. Let $u \in H^2(0,l)$ be an arbitrary function satisfying the boundary conditions $u(0) = u'(0) = 0$. Since $u = \Re(u) + i\Im(u)$, we carry out the proof for the real part $\Re(u)$ only. For convenience, we denote $u = \Re(u)$ and $v = u\exp(-\lambda x)$. In this case, it is sufficient to assume that $u \in C^2[0,l]$ taking into account that the set $C^2[0,l]$ is dense in $H^2(0,l)$. Then we obtain

$$u' = (v' + \lambda v)\exp(\lambda x), \quad u'' = (v'' + 2\lambda v' + \lambda^2 v)\exp(\lambda x).$$

Hence,

$$\begin{aligned}(u'')^2(1+x)^{-1}\exp(-2\lambda x) &= \left[(v'' + \lambda v) + 2\lambda v'\right]^2 (1+x)^{-1} \geqslant 4\lambda v'(v'' + \lambda^2 v)(1+x)^{-1} \\ &= 2\frac{d}{dx}\left[(\lambda(v')^2 + \lambda^3 v^2(1+x)^{-1})\right] + 2[\lambda(v')^2 + \lambda^3 v^2](1+x)^{-2} \\ &\geqslant 2\lambda^3 u^2 (1+x)^{-2}\exp(-2\lambda x) + 2\frac{d}{dx}\left[(\lambda(v')^2 + \lambda^3 v^2(1+x)^{-1})\right].\end{aligned} \tag{49}$$

Integrating (49) with respect to x from 0 to l and taking into account the boundary conditions $u(0) = u'(0) = 0$, we obtain

$$\int_0^l (u'')^2 (1+x)^{-1}\exp(-2\lambda x)\, dx \geqslant 2\lambda^3 \int_0^l u^2 (1+x)^{-2}\exp(-2\lambda x)\, dx. \tag{50}$$

Since $(1+l)^{-1} \leqslant (1+x)^{-1} \leqslant 1$, the inequality (50) implies

$$\int_0^l (u'')^2 \exp(-2\lambda x)\, dx \geqslant \frac{2\lambda^3}{(1+l)^2} \int_0^l u^2 \exp(-2\lambda x)\, dx.$$

This concludes the proof of Lemma 2.

Below by C we denote different positive constants independent of M, Ω, λ, and h. We also denote $p'_{i-1}(\omega) = p'_{i-1}(\xi_{i-1}, p''_{i-1}(\omega) = p''_{i-1}(\xi_{i-1}\omega)$, $p'_0 = 0$, and

$$I_0(\lambda, h) = \frac{1 - \exp(-\lambda h)}{\lambda} = \int_0^h \exp(-\lambda x)\, dx, \quad \lambda > 0. \tag{51}$$

Lemma 3. *Assume that the functions φ, $\dfrac{d\varphi}{d\omega} \in \tilde{G}(M/2)$ and $p'_{i-1}(\omega), p''_{i-1}(\omega) \in \tilde{G}(M)$ $(i = 1, \ldots, n-1)$. Let $J_{\lambda,i}(a_i)$ be the functionals defined by (36). Then the functional $J_{\lambda,i}(a_i)$ can be represented in the form*

$$J_{\lambda,i}(a_i) = I_0(\lambda, h)\left[\int_1^\Omega \left|a_i(\omega) - F_i(\omega)\right|^2 d\omega + \frac{1}{\lambda}\int_1^\Omega H_i(\lambda,\omega)\, d\omega\right] \quad \forall a_i \in \tilde{G}(M),\ \forall \lambda > 1, \tag{52}$$

where

$$F_i(\omega) = F(\omega) + \int_1^\Omega p'_{i-1}(\tau)\, d\tau \cdot \left[2\omega p'_{i-1}(\omega) - \int_1^\Omega p'_{i-1}(\tau)\, d\tau + 2\frac{d\varphi(\omega)}{d\omega}\right] - 2\varphi p'_{i-1}, \tag{53}$$

and the real-valued function H_i satisfies the inequality

$$\|H_i(\lambda,\omega)\|_{C[1,\Omega]} \leqslant C(\Omega M)^4 \quad \forall\lambda \geqslant 1,\ \forall a_i \in \tilde{G}(M). \tag{54}$$

Remark 4.4. It is proven in Theorem 2 (see Section 5) that the functions $p'_{i-1}(\omega)$, $p''_{i-1}(\omega) \in \tilde{G}(M)$.

Proof. Let $1 \leqslant i \leqslant n-2$. Taking into account (32) and (33), we represent the residual $\hat{L}_\Omega(a_i) - F$ in the form

$$\hat{L}_\Omega(a_i) - F = (a_i - F_i)(\omega) + (\xi - \xi_{i-1})\hat{F}_i(a_i, \xi - \xi_{i-1}, \omega), \tag{55}$$

where the function $\hat{F}_i$ is

$$\hat{F}_i(a_i, \xi - \xi_{i-1}, \omega) = \int_1^\Omega a_i(\tau)\,d\tau \cdot \left[-2\omega(\xi - \xi_{i-1})a_i - 2\omega p'_{i-1} + (\xi - \xi_{i-1})\int_1^\Omega a_i(\tau)\,d\tau - 2\,\frac{d\varphi}{d\omega}\right] + 2\varphi a_i. \tag{56}$$

It follows from (56) that

$$\|\hat{F}_i\|_{C^1_\Omega[\xi_{i-1}\xi_i]} \leqslant C(\Omega M)^2 \quad \forall a_i \in \tilde{G}(M). \tag{57}$$

Introduce the moments I_k of CWFs by

$$I_k(\lambda, h) = \int_0^h \xi^k \exp(-\lambda\xi)\,d\xi \quad (k = 1, 2). \tag{58}$$

Since $I_k = (-1)^k d^k I_0/d\lambda^k$, it follows from (51) that

$$\frac{I_k(\lambda,h)}{I_0(\lambda,h)} \leqslant C/\lambda^k \quad (k = 1,2) \quad \forall\lambda \geqslant 1,\ \forall h > 0. \tag{59}$$

Then (55) – (59) imply (52) – (54). The case $i = n-1$ can be considered by analogy.

Thus, Lemma 3 is proved.

Theorem 1. *Let all the conditions of Lemma 3 be satisfied and the functions $F_i \in \tilde{G}(\frac{3}{4}M)$ $(i = 1, \ldots, n-1)$. Then there exists a sufficiently large $\lambda_0 \geqslant C(\Omega M)^4$ such that for all $\lambda \geqslant \lambda_0$ every functional $J_{\lambda,i}(a_i)$ is strictly convex on the set $\tilde{G}(M)$, i.e., $\forall a, b \in \tilde{G}(M)$ the following inequality holds:*

$$J_{\lambda,i}(b) - J_{\lambda,i}(a) - J'_{\lambda,i}(a)(b-a) \geqslant I_0(\lambda,h)\rho\|a-b\|^2_{L_2(1,\Omega)}. \tag{60}$$

Here $\rho \in (1/2, 1)$ is the parameter of strict convexity independent of M, Ω, λ, and h and $J'_{\lambda,i}$ is the Frechét derivative of $J_{\lambda,i}$.

Proof. Let $1 \leqslant i \leqslant n-2$. Let $a(\omega)$ and $b(\omega)$ be two arbitrary functions belonging to the set $\tilde{G}(M)$, $c = b - a$, and

$$q_i(\xi,\omega) = \frac{1}{2}\,b(\omega)(\xi - \xi_{i-1})^2 + p'_{i-1}(\omega)(\xi - \xi_{i-1}) + p_{i-1}(\omega).$$

It follows from (55) and (56) that

$$\begin{aligned}|\hat{L}_\Omega(q_i) - F|^2 = |a + c - F_i|^2 + 2(\xi - \xi_{i-1}) \cdot \Re\big[(a + c - F_i) \cdot \overline{\hat{F}_i}(a + c, \xi - \xi_{i-1}, \omega)\big] \\ + (\xi - \xi_{i-1})^2 \cdot \big|\hat{F}_i(a + c, \xi - \xi_{i-1}, \omega)\big|^2,\end{aligned} \tag{61}$$

where $\overline{\hat{F}_i}$ means the complex-conjugate quantity. Then we obtain from (56)

$$\begin{aligned}|\hat{L}_\Omega(q_i) - F|^2 = |a - F_i|^2 + 2\Re\big[c(\overline{a} - \overline{F_i})\big] + |c|^2 + (\xi - \xi_{i-1})S_1(a, c, \xi - \xi_{i-1}, \omega) \\ + (\xi - \xi_{i-1})S_2(a, c, \xi - \xi_{i-1}, \omega),\end{aligned} \tag{62}$$

where S_1 and S_2 are the linear and nonlinear operators acting on the vector $c = (\Re(c), \Im(c))$. Below we denote by $\overline{a}$, $\overline{c}$, $\overline{p}'_{i-1}$, and $\overline{\varphi}$ the complex conjugate of a, c, p'_{i-1}, and φ. The operators S_1 and S_2 have the forms

$$S_1(a,c,\xi-\xi_{i-1},\omega) = 2\Re\Bigg\{c\cdot\overline{\hat{F}}_i(a,\xi-\xi_{i-1},\omega) + (a-F_i)\times$$
$$\Bigg\{\int_\omega^\Omega \overline{c}\,d\tau\Bigg[-2(\xi-\xi_{i-1})\omega\overline{a} - 2\omega\overline{p}'_{i-1} + 2(\xi-\xi_{i-1})\int_\omega^\Omega \overline{a}\,d\tau - 2\,\frac{d\overline{\varphi}}{d\omega}\Bigg] + 2\overline{\varphi c}\Bigg\}\Bigg\}$$
$$+2\Re\Bigg\{\Bigg\{\int_\omega^\Omega \overline{c}\,d\tau\cdot\Bigg[-2(\xi-\xi_{i-1})\omega a - 2\omega p'_{i-1} + 2(\xi-\xi_{i-1})\times \tag{63}$$
$$\int_\omega^\Omega \overline{a}\,d\tau - 2\,\frac{d\varphi}{d\omega}\Bigg] + 2\varphi c\Bigg\}\cdot\overline{\hat{F}}_i(a,\xi-\xi_{i-1},\omega)\Bigg\},$$

$$S_2(a,c,\xi-\xi_{i-1},\omega) = 2\Re\Bigg\{(a-F_i)\cdot\Bigg(\int_\omega^\Omega \overline{c}\,d\tau\Bigg)^2(\xi-\xi_{i-1})$$
$$+c\Bigg\{\int_\omega^\Omega \overline{c}\,d\tau\cdot\Bigg[-2(\xi-\xi_{i-1})\omega\overline{a} - 2\omega\overline{p}'_{i-1}$$
$$+2(\xi-\xi_{i-1})\int_\omega^\Omega \overline{a}\,d\tau - 2\,\frac{d\overline{\varphi}}{\omega}\Bigg] + 2\overline{\varphi c} + \Bigg(\int_\omega^\Omega \overline{c}\,d\tau\Bigg)^2(\xi-\xi_{i-1})\Bigg\}\Bigg\}$$
$$+2\Re\Bigg\{\Bigg(\int_\omega^\Omega c\,d\tau\Bigg)^2\overline{\hat{F}}_i(a,\xi-\xi_{i-1},\omega)(\xi-\xi_{i-1})\Bigg\} \tag{64}$$
$$+\Bigg|\int_\omega^\Omega c\,d\tau\cdot\Bigg[-2(\xi-\xi_{i-1})\cdot\omega a - 2\omega p'_{i-1} + 2(\xi-\xi_{i-1})\int_\omega^\Omega a\,d\tau - 2\,\frac{d\overline{\varphi}}{\omega}\Bigg]$$
$$+2\varphi c + \Bigg(\int_\omega^\Omega c\,d\tau\Bigg)^2(\xi-\xi_{i-1})\Bigg|^2.$$

From (57) and (64) we then obtain

$$\left|\frac{\partial^j}{\partial\xi^j}S_2\right| \leqslant C(\Omega M)^4\big|c(\omega)\big|^2 \quad \forall a,b\in\tilde{G}(M),\ \forall c = b-a \quad (j=1,2). \tag{65}$$

It follows from (58), (59), and (61)–(65) that for all $a, b \in \tilde{G}(M)$, $c = b - a$, and $\lambda \geqslant 1$ the following estimate holds:

$$J_{\lambda,i}(b) - J_{\lambda,i}(a) - J'_{\lambda,i}(a)(b-a) \geqslant I_0(\lambda,h)\big[1+\lambda^{-1}S_3(c,\lambda)\big]\int_1^\Omega |c|^2\,d\tau, \tag{66}$$

where the functional $S_3(c,\lambda)$ satisfies the inequality

$$\big|S_3(c,\lambda)\big| \leqslant C(\Omega M)^4.$$

Choosing a value of λ such that $C(\Omega M)^4\lambda^{-1} \leqslant \gamma$, $\gamma \in (0, 1/2)$, we obtain from (66)

$$J_{\lambda,i}(b) - J_{\lambda,i}(a) - J'_{\lambda,i}(a)(b-a) \geqslant I_0(\lambda,h)\Bigg[(1-\gamma)\int_1^\Omega |a-b|^2\,d\tau\Bigg]. \tag{67}$$

The case $i = n-1$ can be considered by analogy.

Thus, Theorem 1 is proved.

5. Stability analysis. In Section 3.2, we have introduced the function p^* corresponding to the "exact" solution σ^* of Inverse Problem I. However, the sequential minimization algorithm results in a certain function $\tilde{p}$ that generates the solution $\tilde{\sigma}$ to Inverse Problem II. It is clear that $\tilde{\varepsilon} \to 0$ as $\Omega \to \infty$. In practice, both the parameters $\tilde{\varepsilon}$ and δ and the frequency Ω may vary in broad ranges. Under these conditions, the sequential minimization algorithm requires the stability analysis. In other words, the continuous dependence of a certain norm $\|\tilde{p} - p^*\|$ on δ, $\tilde{\varepsilon}$, and the step size h must be rigorously justified. In this section, we establish such a dependence. We first prove three lemmas.

Lemma 4. *For any complex-valued function $s \in C[1,\Omega]$, the Frechét derivative of the functional $J_{\lambda,i}(a_i)$ $(i = 1, 2, \ldots, n-2)$ is given by*

$$J'_{\lambda,i}(a_i)(s) = I_0(\lambda,h)\cdot 2\Re\left[\int_1^\Omega \overline{s}(\omega)(a_i - F_i)\,d\omega\right] + 2\Re\left\{\int_1^\Omega s(\omega)\big(1+2\varphi(\omega)\big)\cdot\int_{\xi_{i-1}}^{\xi_i}(\xi-\xi_{i-1})\,C^2_{\lambda,i}(\xi)\right.$$
$$\times\left\{\int_\omega^\Omega \overline{a}_i(\tau)\,d\tau\left[-2(\xi-\xi_{i-1})\omega\overline{a}_i - 2\omega p'_{i-1} + (\xi-\xi_{i1})\int_\omega^\Omega \overline{a}_i(\tau)\,d\tau - 2\,\frac{d\overline{\varphi}}{d\omega}\right] + 2\overline{\varphi a}_i\right\}d\xi\,d\omega\Big\}$$
$$+2\Re\left\{\int_1^\Omega s(\omega)\int_{\xi_{i-1}}^{\xi_i}(\xi-\xi_{i-1})\,C^2_{\lambda,i}(\xi)\cdot\int_1^\omega d\tau\left\{(\overline{a}_i-\overline{F}_i)\left[-2(\xi-\xi_{i-1})\tau\overline{a}_i - 2\tau p'_{i-1}\right.\right.\right.$$
$$\left.\left.\left.+2(\xi-\xi_{i-1})\int_\tau^\Omega a_i(\nu)\,d\nu - 2\,\frac{d\varphi}{d\omega}\right]\right\}d\xi\,d\omega\Big\} + 2\Re\left\{\int_1^\Omega s(\omega)\int_{\xi_{i-1}}^{\xi_i}(\xi-\xi_{i-1})\,C^2_{\lambda,i}(\xi)\right.$$
$$\left.\times\int_1^\omega d\tau\left\{\left[-2(\xi-\xi_{i-1})\tau\overline{a}_i - 2\tau p'_{i-1} + 2(\xi-\xi_{i-1})\int_\tau^\Omega a_i(\nu)\,d\nu - 2\,\frac{d\varphi}{d\omega}\right]\cdot\overline{\hat{F}}(a_i,\xi-\xi_{i-1},\tau)\right\}d\xi\,d\omega\right\},$$

where $\hat{F}$ is defined by (56) *and a horizontal bar over variables means the complex conjugation.*

Proof. The proof follows from (36), (62), and (63).

Remark 5.1. A similar formula for $J_{\lambda,(n-1)}(a_{n-1})$ can be obtained in the same way.

Lemma 5. *Suppose the functions φ, $\dfrac{d\varphi}{d\omega} \in \tilde{G}(M/2)$ and $p'_{i-1}, p''_{i-1} \in \tilde{G}(M)$, $F_i \in \tilde{G}(\frac{3}{4}M)$. Then there exists a sufficiently large number $\lambda_0 \geqslant C(\Omega M)^4$ such that the functional $J_{\lambda,i}(a_i)$ is strictly convex on the set $\tilde{G}(M)$ for all $\lambda \geqslant \lambda_0$ and the minimization problem*

$$\operatorname{argmin}\big\{J_{\lambda,i}(a_i) : a_i \in \tilde{G}(M)\big\} \tag{68}$$

is uniquely solvable, whereas the minimizer $\tilde{a}_i$ is an interior point of $\tilde{G}(M)$. This minimizer is a solution to an operator equation $a_i = A_i a_i$ with a contraction operator $A_i : \tilde{G}(M) \to \tilde{G}(M)$.

Proof. Because of (60), it is sufficient to show that for a sufficiently large $\lambda \geqslant \lambda_0 \geqslant C(\Omega M)^4$ the equation

$$J'_{\lambda,i}(a_i)(s) = 0 \quad \forall s \in \tilde{G}(M) \tag{69}$$

has a unique solution belonging to the interior of $\tilde{G}(M)$. Let $1 \leqslant i \leqslant n-2$. Lemma 3, (51), (58), and (59) imply that for any complex-valued function $s \in C[1,\Omega]$ the following equality holds:

$$J'_{\lambda,i}(a_i)(s) = I_0(\lambda,h)\cdot\left[2\Re\int_1^\Omega s(\omega)(\overline{a}_i - \overline{F}_i)\,d\omega - 2\Re\int_1^\Omega s(\omega)\cdot\lambda^{-1}T_i(a_i,\omega,\lambda)\,d\omega\right], \tag{70}$$

where

$$\big\|T_i(a_i,\omega,\lambda)\big\|_{C[1,\Omega]} \leqslant C(\Omega M)^2 \quad \forall a_i \in \tilde{G}(M),\ \forall\lambda \geqslant \lambda_0. \tag{71}$$

We obtain from (69) and (70) the equivalent equation

$$a_i(\omega) = F_i + \lambda^{-1}\overline{T}_i(a_i,\omega,\lambda). \tag{72}$$

Define the map $A_i : C[1,\Omega] \to C[1,\Omega]$ by

$$A_i(a) = F_i + \lambda^{-1}\overline{T}_i(a,\omega,\lambda). \tag{73}$$

We can then rewrite Eq. (72) in the form

$$a_i = A_i(a_i). \tag{74}$$

Choose $\lambda_0 \geqslant C(\Omega M)^4$ such that the following inequality holds:

$$\lambda^{-1}C(\Omega M)^2 < M/4. \tag{75}$$

Since $F_i \in \tilde{G}(\frac{3}{4}M)$, we obtain from (71) – (75)

$$\|A_i(a_i)\|_{C[1,\Omega]} \leqslant \|F_i\|_{C[1,\Omega]} + \frac{M}{4} < \frac{3}{4}M + \frac{M}{4} < M. \tag{76}$$

This inequality implies that

$$A_i : \tilde{G}(M) \to \tilde{G}(M). \tag{77}$$

It follows from Lemma 4 and (70) that

$$\begin{aligned} \|A_i(a_1) - A_i(a_2)\|_{C[1,\Omega]} &\leqslant \lambda^{-1} \big\|T_i(a_1,\omega,\lambda) - T_i(a_2,\omega,\lambda)\big\|_{C[1,\Omega]} \\ &\leqslant \lambda^{-1} C(\Omega M)^2 \|a_1 - a_2\|_{C[1,\Omega]} \quad \forall a_1, a_2 \in \tilde{G}_i(M). \end{aligned} \tag{78}$$

In addition to (75), choose a sufficiently large parameter λ_0 such that for $\lambda \geqslant \lambda_0$

$$\lambda^{-1} C(\Omega M)^2 < 1/2. \tag{79}$$

Then, equations (77)–(79) imply that the map A_i is contractive on the set $\tilde{G}(M)$. The case $i = n-1$ can be considered by analogy.

This concludes the proof of Lemma 5.

Taking into account (see Section 3.2) that the function $\varphi^*(\omega)$ corresponds to the "exact" conductivity distribution $\sigma^*(\xi)$, we shall call $\varphi^*(\omega)$ the "exact" sounding data. In addition we denote

$$F^*(\omega) = \frac{\varphi^*(\omega)}{\omega}\left[\frac{\varphi^*(\omega)}{\omega} - 2\,\frac{d\varphi^*(\omega)}{d\omega}\right], \tag{80}$$

$$L^*_\Omega(p^*,\varphi^*) = p^{*\prime\prime} - 2\omega p^{*\prime}\int_\omega^\Omega p^{*\prime} d\tau + \left(\int_\omega^\Omega p^{*\prime} d\tau\right)^2 - 2\,\frac{d\varphi^*(\omega)}{d\omega}\int_\omega^\Omega p^{*\prime} d\tau + 2\varphi^* p^{*\prime}, \tag{81}$$

$$\Delta F = F - F^*,\ \Delta\varphi = \varphi - \varphi*. \tag{82}$$

By analogy with (53), we denote

$$F_i^*(\omega) = F^*(\omega) + \int_1^\Omega p^{*\prime}_{i-1}(\tau)\,d\tau \cdot \left[2\omega p^{*\prime}_{i-1}(\omega) - \int_1^\Omega p^{*\prime}_{i-1}(\tau)\,d\tau + 2\,\frac{d\varphi^*(\omega)}{d\omega}\right] - 2\varphi^* p^{*\prime}_{i-1}. \tag{83}$$

Then, we have $F_1^* = F^*$. Furthermore, let us denote $\varepsilon = |(\tilde{\varepsilon},\delta)|$. Without loss of generality, assume that the following inequalities are fulfilled:

$$\|\Delta F\|_{C[1,\Omega]} < \frac{\varepsilon}{4}, \tag{84}$$

$$\big\|L^*_\Omega(p^*,\varphi^*) - F^*\big\|_{C[1,\Omega]} < \frac{\varepsilon}{4}, \tag{85}$$

$$\|\Delta\varphi\|_{C^1[1,\Omega]} < \frac{\varepsilon}{4}. \tag{86}$$

Also, denote $(p^*_{i-1})^{(s)}(\omega) = (p^*_{i-1})^{(s)}(\xi_{i-1},\omega)$, $s = 1, 2$, $1 \leqslant i \leqslant n$.

Lemma 6. *Let $p^* \in G(M/2)$ and the inequalities (84)–(86) hold. Then the following inequality holds:*

$$\|F_i^*\|_{C[1,\Omega]} \leqslant \frac{M}{2} + \frac{\varepsilon}{4}, \quad i = 1,\ldots,n-1. \tag{87}$$

Proof. Let $1 \leqslant i \leqslant n-2$. We have from (81) and (83)

$$L^*_\Omega\big(p^*(\xi_{i-1},\omega),\varphi^*\big) - F^*(\omega) = (p^*_{i-1})''(\omega) - F_i^*(\omega). \tag{88}$$

The inequality (85) implies that $\|F_i^*\|_{C[1,\Omega]} \leqslant \varepsilon/4 + \|(p^*)''_{i-1}\|_{C[1,\Omega]}$. Since $p^* \in G(M/2)$, we obtain the inequality (87) from (88). The case $i = n-1$ can be considered by analogy.

Thus, Lemma 6 is proved.

Theorem 2. *Let $\sigma^*(\xi) \geqslant \mathrm{const} > 0$ be a bounded piecewise continuous function on $[0,1]$, $p^* \in G(M/2)$, and the inequalities (84)–(86) hold. Let $\lambda_0 \geqslant C(\Omega M)^4$ be a sufficiently large parameter such that for $\lambda \geqslant \lambda_0$ the inequalities (75) and (79) hold and*

$$\lambda^{-1} C(\Omega M)^2 < \frac{\varepsilon}{2}. \tag{89}$$

For such λ, let $\{\tilde{p}_i(\xi,\omega)\}_{i=1}^{i=n}$ be the sequence of functions corresponding to the coefficients $\tilde{a}_i$ determined via the procedure of sequential minimization, i.e., the functions $\tilde{p}_i(\xi,\omega)$ are determined from Eqs (33) and (34). Then there exist sufficiently small numbers $\varepsilon_0 = \varepsilon_0(\Omega, M) > 0$, $h_0 = h_0(\Omega, M) > 0$ such that for all $\varepsilon \in (0, \varepsilon_0)$, $h \in (0, h_0)$ the functions

$$\tilde{p}'_{i-1}(\xi_{i-1},\omega)\ \tilde{p}''_{i-1}(\xi_{i-1},\omega) \in \tilde{G}(M) \quad (i = 1,\dots,n-1), \tag{90}$$

$$F_i \in \tilde{G}\left(\frac{3}{4}M\right) \quad (i = 1,\dots,n-1) \tag{91}$$

and the following estimates hold:

$$\|\Delta p_i^{(s)}\|_{C[1,\Omega]} \leqslant K(\varepsilon + h), \quad s = 0,1,2, \quad i = 1,\dots,n-1, \tag{92}$$

Here

$$\Delta p_i^{(s)}(\omega) = \frac{\partial^{(s)}}{\partial \xi^{(s)}}\left[\tilde{p}_i(\xi_{i-1},\omega) - p^*(\xi_{i-1},\omega)\right], \tag{93}$$

$\tilde{p}_0(\xi_0,\omega) = \tilde{p'}_0(\xi_0,\omega) = 0$, $\tilde{p''}_0(\xi_0,\omega) = \tilde{a}_1(\omega)$, *and $K = K(\Omega, M) > 0$ is a constant depending on Ω and M. However, this constant does not depend on ε, λ, and h.*

Remark 5.2. It follows from Lemma 5 and Theorem 2 that $\tilde{G}(M)$ is a correctness set for the minimization problems (37) – (38). This means that these problems are conditionally well-posed on $\tilde{G}(M)$ according to the concepts and definitions indicated in [24, 26, 27]. In other words, the specific forms of the objective functions $J_{\lambda,i}(a_i)$ and the feasible region $\tilde{G}(M)$ for unknowns $a_i(\omega)$ allow us to regularize the originally ill-posed p-field prediction problem.

Remark 5.3. Without loss of generality, we assume below that $\Omega \geqslant 1$, $M \geqslant 1$.

Proof. In this proof we assume that $\|\cdot\| = \|\cdot\|_{C[1,\Omega]}$. The mathematical induction is used to prove the theorem. Let $i = 1$. Then we obtain from (32) $p_1 = a_1(\omega)\frac{\xi^2}{2}$, $\xi \in (\xi_0, \xi_1]$. Since $F_1^* = F^*$, we have from (84) and (85) $\|F_1\| < \frac{(M+\varepsilon)}{2} < \frac{3}{4}M$, where $F_1 = F$ and $\varepsilon < \varepsilon_0 < M/2$. This means that $F_1 \in \tilde{G}(3M/4)$. This fact proves (91) for $i = 1$. It follows from Theorem 1 and Lemma 5 that the functional $J_{\lambda,1}$ is strictly convex on $\tilde{G}(M)$ and its unique minimizer $\tilde{a}_1$ belongs to the interior of $\tilde{G}(M)$. On the other hand, due to (72), this minimizer is the unique solution of the equation

$$\tilde{a}_1(\omega) = F_1 + \lambda^{-1}\overline{T}_1(\tilde{a}_1,\omega,\lambda). \tag{94}$$

Denote $g_\varepsilon^*(\xi,\omega) = L_\Omega(p^*,\varphi^*) - F^*$. From (85), then, we have

$$\left\|g_\varepsilon^*(\xi,\omega)\right\|_{C_\Omega[0,1]} < \frac{\varepsilon}{4}. \tag{95}$$

From (88) we have $(p_0^*)'' = F_1^* + g_\varepsilon^*(0,\omega)$. Using Taylor's formula, we obtain

$$p^*(\xi,\omega) = a_1^*(\omega)\,\frac{\xi^2}{2} + \frac{1}{2}\int_0^\xi (\xi - \xi')^2 p^{*(3)}(\xi',\omega)\,d\xi', \quad \xi \in (\xi_0,\xi_1), \tag{96}$$

where $a_1^* = F_1^* + g_\varepsilon^*(0,\omega)$. Denoting $\Delta a_1 = \tilde{a}_1 - a_1^*$ and $\Delta F_1 = F_1 - F^*$, from (94) we obtain

$$\Delta a_1 = \Delta F_1 + \lambda^{-1}\overline{T}_1(\tilde{a}_1,\omega,\lambda) - g_\varepsilon^*(0,\omega). \tag{97}$$

It follows from (71), (84), (89), (95), and (97) that

$$\|\Delta a_1\| \leqslant \frac{\varepsilon}{4} + \frac{\varepsilon}{2} + \frac{\varepsilon}{4} = \varepsilon. \tag{98}$$

Using (96) and (98), we obtain

$$\Delta p_2' = (p_1' - p^{*\prime})(\xi_1,\omega) = \Delta a_1 \cdot h - \int_0^h (h - \xi')p^{*(3)}(\xi',\omega)\,d\xi'.$$

Since $p^* \in G(M/2)$, from (98) we then obtain

$$\|\Delta p_2'\| \leqslant \varepsilon h + Mh^2/4. \tag{99}$$

Noticing that $\Delta p_2 = \Delta a_1 \cdot h^2/2 + \Delta p'_2 \cdot h$, from (98) and (99) we get

$$\|\Delta p_2\| \leqslant \frac{3}{2}\,\varepsilon h^2 + Mh^3/4. \tag{100}$$

The estimate (92) for $i = 2$ follows immediately from (93), (98), (99), and (100). For $i = 1$, it is obvious, since $\Delta p_1 = \Delta p'_1 = 0$, $\Delta p''_1 = \Delta a_1$, and (98) holds.

Since $p'_1(\xi_1, \omega) = \Delta p'_2(\omega) + p^{*'}(\xi_1, \omega)$ and $p^* \in G(M/2)$, then (99) implies

$$\|p'_1\| \leqslant \frac{M}{2} + \varepsilon h + \frac{M}{4}\,h^2. \tag{101}$$

In addition, it follows from (98) that

$$\|a_1\| < \frac{M}{2} + \varepsilon. \tag{102}$$

Assume that the following inequalities hold:

$$\varepsilon h + \frac{M}{4}h^2 < \frac{M}{2} \quad \forall (\varepsilon, h) \in (0, \varepsilon_0) \times (0, h_0), \tag{103}$$

$$\varepsilon < \frac{M}{2} \quad \forall \varepsilon \in (0, \varepsilon_0) \subset (0, 1). \tag{104}$$

Then, the inequalities (101) and (102) imply

$$\tilde{p'}_1(\xi_1, \omega),\ \tilde{p''}_1(\xi_1, \omega) \in \tilde{G}(M). \tag{105}$$

Since $\tilde{p'}_1(\xi_0, \omega) = 0$, $\tilde{p''}_0(\xi_0, \omega) = \tilde{a}_1(\omega)$, then (105) establishes (90) for $i = 1, 2$. To prove (91) for $i = 2$, consider the quantity $\Delta F_i = F_i - F_i^*$. By virtue of (53) and (83), we have

$$\begin{aligned}\Delta F_i = \Delta F_1 &+ \int_\omega^\Omega \Delta p'_i(\tau)\,d\tau \cdot \left[2\omega p^{*'}_{i-1}(\omega) - \int_\omega^\Omega p^{*'}_{i-1}(\tau)\,d\tau + 2\,\frac{d\varphi^*}{d\omega}\right] \\ &+ \int_\omega^\Omega \tilde{p'}_{i-1}(\tau)\,d\tau \cdot \left[2\omega \Delta p'_i - \int_\omega^\Omega \Delta p'_{i-1}(\tau)\,d\tau + 2\Delta \frac{d\varphi}{d\omega}\right] - 2\Delta\varphi \cdot p^{*'}_{i-1} - 2\varphi \Delta p_i.\end{aligned} \tag{106}$$

Assuming $i = 2$ in (106) and taking account of (84), (86), (99), and (105), we obtain

$$\|\Delta F_2\| \leqslant \frac{\varepsilon}{4}(1 + 2\Omega M + M) + \|\Delta p'_2\| \cdot (5\Omega^2 M + 3M) \leqslant 8\Omega^2 M(\varepsilon + \varepsilon h + Mh^2). \tag{107}$$

Applying (87), we get

$$\|F_2\| \leqslant \frac{M}{2} + \frac{\varepsilon}{4} + 8\Omega^2 M(\varepsilon + \varepsilon h + Mh^2). \tag{108}$$

Assume that in addition to (103) and (104), the following inequality holds:

$$\frac{\varepsilon}{4} + 8\Omega^2 M(\varepsilon + \varepsilon h + Mh^2) < \frac{M}{5} \quad \forall (\varepsilon, h) \in (0, \varepsilon_0) \times (0, h_0). \tag{109}$$

Then the inequality (108) implies $\|F_2\| < M/2 + M/5 < 3M/4$, which establishes (91) for $i = 2$.

Let $2 \leqslant k \leqslant n - 2$. Assume that (90) hold for $1 \leqslant j \leqslant k - 1$ and (91), (92) hold for $1 \leqslant j \leqslant k$ and $s = 1, 2$. We shall establish (90) for $j = k$ and (91), (92) for $j = k + 1$.

It follows from Lemma 4 that the unique minimizer $\tilde{a}_k$ of the functional $J_{\lambda,k}(a_k)$ belongs to the interior of $\tilde{G}(M)$ and satisfies the equation

$$\tilde{a}_k(\omega) = F_k(\omega) + \lambda^{-1}\overline{T}_k(\tilde{a}_k, \omega, \lambda). \tag{110}$$

Representing the function $p^*(\xi, \omega)$ via Taylor's formula, we obtain

$$\begin{aligned}p^*(\xi, \omega) = a_k^*(\omega)\,\frac{(\xi - \xi_{k-1})^2}{2} &+ p^{*'}(\xi_{k-1}, \omega)(\xi - \xi_{k-1}) + p^*(\xi_{k-1}, \omega) \\ &+ \frac{1}{2}\int_{\xi_{k-1}}^{\xi} (\xi - \xi')^2 p^{*(3)}(\xi', \omega)\,d\xi', \quad \xi \in (\xi_{k-1}, \xi_k).\end{aligned} \tag{111}$$

Therefore, equations (81) and (83) imply

$$a_k^*(\omega) = p^{*\prime\prime}(\xi_{k-1}, \omega) = g_\varepsilon^*(\xi_{k-1}, \omega) + F_k^*(\omega). \tag{112}$$

Subtracting (112) from (110) and denoting $\Delta a_k = \tilde{a}_k - a_k^*$, we come to the equality

$$\Delta a_k = \Delta F_k + \lambda^{-1}\overline{T}_k(\tilde{a}_k, \omega, \lambda) - g_\varepsilon^*(\xi_{k-1}, \omega). \tag{113}$$

It follows from (71), (89), and (95) that

$$\|\Delta a_k\| \leqslant \|\Delta F_k\| + \frac{\varepsilon}{2} + \frac{\varepsilon}{4} \leqslant \|\Delta F_k\| + \frac{3}{4}\,\varepsilon. \tag{114}$$

From (84), (86), and (106) we obtain

$$\|\Delta F_k\| \leqslant (2\Omega M)\cdot\varepsilon + 9(\Omega^2 M)\cdot\|\Delta p_k'\|. \tag{115}$$

Hence, the inequality (114) implies

$$\|\Delta a_k\| \leqslant (3\Omega M)\cdot\varepsilon + 9(\Omega^2 M)\cdot\|\Delta p_k'\|. \tag{116}$$

It follows from (33) that $\tilde{p}_k'(\xi_k, \omega) = \tilde{a}_k \cdot h + \tilde{p}_{k-1}'(\xi_{k-1}, \omega)$. Hence, the equations (93), (111) imply

$$\Delta p_{k+1}' = \Delta a_k \cdot h + \Delta p_k' - \int_{\xi_{k-1}}^{\xi_k} (\xi_k - \xi')p^{*(3)}(\xi', \omega)\,d\xi',$$

$$\|\Delta p_{k+1}'\| \leqslant \|\Delta a_k\|\cdot h + \|\Delta p_k'\| + \frac{Mh^2}{4}.$$

Taking into account (116), we then obtain

$$\|\Delta p_{k+1}'\| \leqslant (3\Omega M)\cdot(\varepsilon h + h^2) + \big[1 + 9(\Omega^2 M)h\big]\cdot\|\Delta p_k'\|. \tag{117}$$

Under our assumptions, this inequality holds for all j such that $2 \leqslant j \leqslant (k-1)$. Hence, we obtain

$$\|\Delta p_{k+1}'\| \leqslant (3\Omega M)\cdot(\varepsilon h + h^2)\cdot\sum_{j=0}^{k-1}\big[1 + 9(\Omega^2 M)h\big]^j + \big[1 + 9(\Omega^2 M)h\big]^{k-1}\cdot\|\Delta p_2'\|. \tag{118}$$

Noticing that the first term in the right-hand side of (118) is proportional to the sum of geometrical progression, we come to the estimate

$$(3\Omega M)\cdot(\varepsilon h + h^2)\cdot\sum_{j=0}^{k-1}\big[1 + 9(\Omega^2 M)h\big]^j \leqslant (\varepsilon + h)\big[1 + 9(\Omega^2 M)h\big]^k. \tag{119}$$

Since $h = 1/(n-1)$ and $k \leqslant (n-2)$, we get

$$\big[1 + 9(\Omega^2 M)h\big]^{k-1} < \exp\big[9\Omega^2 M\big]. \tag{120}$$

The inequalities (99), (119), and (120) imply that

$$\|\Delta p_{k+1}'\| \leqslant \exp\big[9(\Omega^2 M)\big](2\varepsilon + h + \varepsilon h + Mh^2). \tag{121}$$

Assume that

$$(M + 1/2)h^2 < h \quad \forall h \in (0, h_0). \tag{122}$$

Since $\varepsilon < 1$ (see (104)), it follows from (121) that

$$\|\Delta p'_{k+1}\| \leqslant 3\exp\big[9(\Omega^2 M)\big](\varepsilon + h). \tag{123}$$

Since $\Delta p_{k+1}'' = \Delta a_k$, then the inequalities (116) and (123) imply

$$\begin{aligned}\|\Delta p_{k+1}''\| &\leqslant (3\Omega M)\cdot\varepsilon + 27(\Omega^2 M)\exp\big[9(\Omega^2 M)\big](\varepsilon + h)\\ &\leqslant 28(\Omega^2 M)\exp\big[9(\Omega^2 M)\big]\cdot(\varepsilon + h).\end{aligned} \tag{124}$$

Finally, noticing that $\Delta p_{k+1} = \Delta a_k \cdot h^2/2 + \Delta p'_k \cdot h + \Delta p_k$ and

$$\Delta p_{k+1} = \frac{h^2}{2}\sum_{j=1}^{k}\Delta a_j + h\sum_{j=1}^{k}\Delta p'_j,$$

from (123) and (124) we obtain

$$\begin{aligned}\|\Delta p_{k+1}\| &\leqslant 28(\Omega^2 M)\exp\left[9(\Omega^2 M)\right]\cdot(\varepsilon+h)\cdot\left(\frac{(n-1)h^2}{2}+(n-1)h\right)\\ &\leqslant 42(\Omega^2 M)\exp\left[9(\Omega^2 M)\right]\cdot(\varepsilon+h).\end{aligned} \tag{125}$$

To prove (90) for $j = k$, we notice that

$$\|\tilde{p}_k^{(s)}\| \leqslant \|p_k^{*(s)}\| + \|\Delta p_{k+1}^{(s)}\| \leqslant \frac{M}{2} + \|\Delta p_{k+1}^{(s)}\|. \tag{126}$$

Since $\tilde{p}''_k = \tilde{a}_k(\omega) \in \tilde{G}(M)$, then (90) holds true for $\tilde{p''}_k(\xi_k,\omega)$. Assume that the parameters $\varepsilon_0(\Omega, M)$ and $h_0(\Omega, M)$ are chosen sufficiently small, so that in addition to (103), (104), (109), and (122), the following inequality holds:

$$\frac{M}{2} + 42\Omega^2 M\exp\left[9\Omega^2 M\right]\cdot(\varepsilon+h) < \frac{3M}{4}\quad \forall(\varepsilon,h)\in(0,\varepsilon_0)\times(0,h_0). \tag{127}$$

Then, it follows from (123) and (126) that $\tilde{p}'_k(\xi_k,\omega) \in \tilde{G}(M)$, i.e., (90) is established for $j = k$.

Show that $F_{k+1} \in \tilde{G}(3M/4)$. It follows from (115), (123), and (127) that

$$\begin{aligned}\|F_{k+1}\| &\leqslant \frac{M}{2} + (2\Omega M)\cdot\varepsilon + 27(\Omega^2 M)\exp\left[9\Omega^2 M\right]\cdot(\varepsilon+h)\\ &\leqslant \frac{M}{2} + 28(\Omega^2 M)\exp\left[9\Omega^2 M\right]\cdot(\varepsilon+h) < \frac{3}{4}M.\end{aligned}$$

Hence, $F_{k+1} \in \tilde{G}(3M/4)$. Since (90) and (91) are established, the estimates (123)–(125) imply (92). For the last subinterval $[\xi_{n-2}, \xi_{n-1}]$, the proof can be carried out by analogy. However, the Neumann condition at $\xi = 1$ should be taken into account in that case.

Thus, Theorem 2 is proved.

Finally, Theorem 3 shows that the estimate (92) implies the analogous estimate for the solution $\tilde{\sigma}(\xi)$ to Inverse Problem II, where $\tilde{\sigma}(\xi)$ is obtained from (44)–(47).

Theorem 3. *Let all the conditions of Theorem 2 are satisfied and the following inequality holds:*

$$\sup_{\xi\in[0,1]}\left[\int_{\Omega}^{\infty}\left|p^{*(s)}(\xi,\tau)\right|d\tau + \left|w_s^{(s)}(\xi,\Omega)\right|\right] < \alpha,\quad s = 1,2. \tag{128}$$

Here $\alpha > 0$ is a sufficiently small constant. Let $\Delta\sigma_i = \tilde{\sigma}(\xi_{i-1}) - \sigma^*(\xi_{i-1})$. Then the following estimate holds:

$$\max_{0\leqslant i\leqslant n}|\Delta\sigma_i| \leqslant \frac{1}{\mu L^2\tilde{\omega}_{\min}}K_1(\varepsilon+h+\alpha). \tag{129}$$

Here $K_1 = K_1(\Omega, M) > 0$ is a constant depending only on Ω and M.

Proof. Recall that

$$\tilde{w'}(\xi,\omega) = -\int_{\omega}^{\Omega}\tilde{p'}(\xi,\nu)\,d\nu + \frac{\varphi(\omega)}{\omega} + w'_s(\xi,\Omega), \tag{130}$$

$$\tilde{w''}(\xi,\omega) = -\int_{\omega}^{\Omega}\tilde{p''}(\xi,\nu)\,d\nu + w''_s(\xi,\Omega), \tag{131}$$

$$w^{*'}(\xi,\omega) = -\int_{\omega}^{\Omega}p^{*'}(\xi,\nu)\,d\nu + \frac{\varphi^*(\omega)}{\omega} - \int_{\Omega}^{\infty}p^{*'}(\xi,\nu)\,d\nu, \tag{132}$$

$$w^{*''}(\xi,\omega) = -\int_{\omega}^{\Omega}p^{*''}(\xi,\nu)\,d\nu - \int_{\Omega}^{\infty}p^{*''}(\xi,\nu)\,d\nu. \tag{133}$$

By analogy with (93), we denote

$$\Delta w_i^{(s)} = \frac{\partial^{(s)}}{\partial \xi^{(s)}} \left[\tilde{p}_i(\xi_{i-1}, 1) - p_i^*(\xi_{i-1}, 1) \right], \quad s = 1, 2.$$

Then it follows from (46) that

$$\mu L^2 \tilde{\omega}_{\min} |\Delta \sigma_i| \leqslant |\Delta w_i''| + |\Delta w_i'| \cdot \left[|\tilde{w}(\xi_{i-1}, 1)| + |w^*(\xi_{i-1}, 1)| \right]. \tag{134}$$

We estimate all terms in the right-hand side of this inequality. Subtracting (133) from (131) and taking into account (92) and (128), we obtain

$$|\Delta w_i''| \leqslant \Omega \cdot K \cdot (\varepsilon + h) + \alpha. \tag{135}$$

Similarly, subtracting (132) from (130) and taking into account (86), we get

$$|\Delta w_i'| \leqslant \Omega \cdot K \cdot (\varepsilon + h) + \alpha + \frac{\varepsilon}{4}. \tag{136}$$

Since $p^* \in G(M/2)$ and $\tilde{p}'(\xi_{i-1}, \omega) \in \tilde{G}(M)$, then taking into account (86), (130), and (132), we come to the inequality

$$\left| \tilde{w}'(\xi_{i-1}, 1) \right| + \left| w^{*'}(\xi_{i-1}, 1) \right| \leqslant \Omega M + 2M + \alpha. \tag{137}$$

The inequalities (134) – (137) imply (129).

This concludes the proof of Theorem 3.

6. Computational experiments. We have performed some computational experiments to demonstrate the feasibility of the proposed algorithm.

6.1. Models. The models used in computational experiments consist of several layers with parallel interfaces (see Figure 1). In all models, the upper layer ($\xi < 0$) contains the air, i.e., a perfect dielectric whose conductivity is assumed to be zero. The inhomogeneous layer ($0 < \xi < 1$) contains the conductive seawater and several sediment layers. The lower layer ($\xi > 1$) contains the homogeneous basement whose conductivity is two order less than the averaged conductivity of the inhomogeneous layer.

In our computational experiments, we use two realistic marine configurations typical for the shallow water Stockholm archipelago, the Baltic sea. Specifically, we adopt the four layer marine configuration

$$\sigma(z) = \begin{cases} 0,\ \mathrm{S} \cdot \mathrm{m}^{-1} & \text{for } z < 0 \\ 0.70,\ \mathrm{S} \cdot \mathrm{m}^{-1} & \text{for } 0 \leqslant z < 47 \text{ m} \\ 0.14,\ \mathrm{S} \cdot \mathrm{m}^{-1} & \text{for } 47 \text{ m} \leqslant z < 93 \text{ m} \\ 0.001,\ \mathrm{S} \cdot \mathrm{m}^{-1} & \text{for } z \geqslant 93 \text{ m} \end{cases} \tag{138}$$

and the five layer marine configuration

$$\sigma(z) = \begin{cases} 0,\ \mathrm{S} \cdot m^{-1} & \text{for } z < 0 \\ 0.70,\ \mathrm{S} \cdot \mathrm{m}^{-1} & \text{for } 0 \leqslant z < 47 \text{ m} \\ 0.32,\ \mathrm{S} \cdot \mathrm{m}^{-1} & \text{for } 47 \text{ m} \leqslant z < 55 \text{ m} \\ 0.19,\ \mathrm{S} \cdot \mathrm{m}^{-1} & \text{for } 55 \text{ m} \leqslant z < 70 \text{ m} \\ 0.001,\ \mathrm{S} \cdot \mathrm{m}^{-1} & \text{for } z \geqslant 70 \text{ m}. \end{cases} \tag{139}$$

Also, we use the realistic parameters in order to construct two more synthetic marine configurations. The third configuration contains a thin highly conductive layer laying on the sediment layer. This thin layer models a mine.

$$\sigma(z) = \begin{cases} 0,\ \mathrm{S} \cdot \mathrm{m}^{-1} & \text{for } z < 0 \\ 0.70,\ \mathrm{S} \cdot \mathrm{m}^{-1} & \text{for } 0 \leqslant z < 46 \text{ m} \\ 10.0,\ \mathrm{S} \cdot \mathrm{m}^{-1} & \text{for } 46 \text{ m} \leqslant z < 47 \text{ m} \\ 0.14,\ \mathrm{S} \cdot \mathrm{m}^{-1} & \text{for } 47 \text{ m} \leqslant z < 93 \text{ m} \\ 0.001,\ \mathrm{S} \cdot \mathrm{m}^{-1} & \text{for } z \geqslant 93 \text{ m}. \end{cases} \tag{140}$$

The fourth configuration contains ten layers. It has been constructed to model the sediment conductivity stratification due to porosity.

$$\sigma(z) = \begin{cases} 0,\ \mathrm{S}\cdot\mathrm{m}^{-1} & \text{for } z < 0 \\ 0.70,\ \mathrm{S}\cdot\mathrm{m}^{-1} & \text{for } 0 \leqslant z < 47\ \mathrm{m} \\ 0.32,\ \mathrm{S}\cdot\mathrm{m}^{-1} & \text{for } 47\ \mathrm{m} \leqslant z < 55\ \mathrm{m} \\ 0.19,\ \mathrm{S}\cdot\mathrm{m}^{-1} & \text{for } 55\ \mathrm{m} \leqslant z < 60\ \mathrm{m} \\ 0.14,\ \mathrm{S}\cdot\mathrm{m}^{-1} & \text{for } 60\ \mathrm{m} \leqslant z < 70\ \mathrm{m} \\ 0.20,\ \mathrm{S}\cdot\mathrm{m}^{-1} & \text{for } 70\ \mathrm{m} \leqslant z < 75\ \mathrm{m} \\ 0.40,\ \mathrm{S}\cdot\mathrm{m}^{-1} & \text{for } 75\ \mathrm{m} \leqslant z < 80\ \mathrm{m} \\ 0.25,\ \mathrm{S}\cdot\mathrm{m}^{-1} & \text{for } 80\ \mathrm{m} \leqslant z < 87\ \mathrm{m} \\ 0.14,\ \mathrm{S}\cdot\mathrm{m}^{-1} & \text{for } 87\ \mathrm{m} \leqslant z < 93\ \mathrm{m} \\ 0.001,\ \mathrm{S}\cdot\mathrm{m}^{-1} & \text{for } z \geqslant 93\ \mathrm{m}. \end{cases} \tag{141}$$

The conductivity of seawater is $0.7\ \mathrm{S}\cdot\mathrm{m}^{-1}$ for all four models.

6.2. Simulation of sounding data. To simulate the sounding data $\varphi(\omega)$, we solve numerically the boundary value problem (9) – (11). Specifically, we reduce this problem to a system of first-order differential equations. This can be accomplished by introducing the new variable

$$y = -\frac{1}{\sqrt{\omega}}\,\frac{u'}{u}.$$

Then we obtain the Cauchy problem for the linear first-order equation

$$u' + \sqrt{\omega}yu = 0, \quad 0 < \xi < 1, \tag{142}$$

$$u(0,\omega) = 1 \tag{143}$$

and the Cauchy problem for the Riccati equation

$$y' = \sqrt{\omega}\big(y^2 - i\mathcal{C}^2\sigma(\xi)\big), \quad 0 < \xi < 1, \tag{144}$$

$$y(1,\omega) = -\mathcal{C}(i+1)\sqrt{\sigma_b/2}, \tag{145}$$

where $\mathcal{C} = L\sqrt{\mu\tilde{\omega}_{\min}}$. Setting $y = y_p + z$, where y_p is the particular solution of the Riccati equation, we obtain the two Cauchy problems with respect to y_p and z

$$y_p' = \sqrt{\omega}\big(y_p^2 - i\mathcal{C}^2\sigma(\xi)\big), \quad 0 < \xi < 1, \tag{146}$$

$$y_p(1,\omega) = -i\mathcal{C}\sqrt{\sigma_b/2} \tag{147}$$

and the Cauchy problem for the Bernoulli equation

$$z' = \sqrt{\omega}(z^2 + 2y_p z), \quad 0 < \xi < 1, \tag{148}$$

$$z(1,\omega) = -\mathcal{C}\sqrt{\sigma_b/2}. \tag{149}$$

Since both the linear (142) and Bernoulli (148) equations are integrated in closed form, the sounding data can be represented as

$$\varphi(\omega) = -\sqrt{\omega}\big[y_p(0,\omega) + t^{-1}(0,\omega)\big], \tag{150}$$

where

$$t(0,\omega) = \sqrt{\omega}\int_0^1 \exp\big(2\sqrt{\omega}\mathcal{I}_1(y_p,\zeta)\big)\,d\zeta - \mathcal{C}^{-1}\sqrt{2/\sigma_b}\exp\big(2\sqrt{\omega}\mathcal{I}_2(y_p,0)\big),$$

$$\mathcal{I}_1(y_p,\zeta) = \int_0^\xi y_p(\zeta,\omega)\,d\zeta, \quad \mathcal{I}_2(y_p,\zeta) = \int_\xi^1 y_p(\zeta,\omega)\,d\zeta,$$

It can be seen from (150) that the function $\varphi(\omega)$ is actually determined by the particular solution y_p to the Riccati equation. We solve numerically the problem (146) – (147) using a fourth-order Runge–Kutta method. Because of algorithmic and roundoff errors, the simulated data are always slightly perturbed. The relative level of the total error has been estimated by testing the Riccati solver against the analytical solutions of the forward

problem for the three and four layer configurations. Based on the test results, we are confident that it does not exceed $5 \cdot 10^{-5}$. Figure 2 shows the comparison between the analytical and numerical solutions in terms of the logarithmic apparent resistivity $\rho_a = \log_{10}[\omega\mu/|\varphi(\omega)|^2]$, which is usually used in practice to represent the data. For the sake of visualization, here and below we display the dimensional frequency $\tilde{f} = \tilde{\omega}/2\pi$. Although such slightly perturbed data are used in all computational experiments, in this paper we do not model the noisy data. Instead, we focus on simulating the incomplete data and extending them to a broader frequency band.

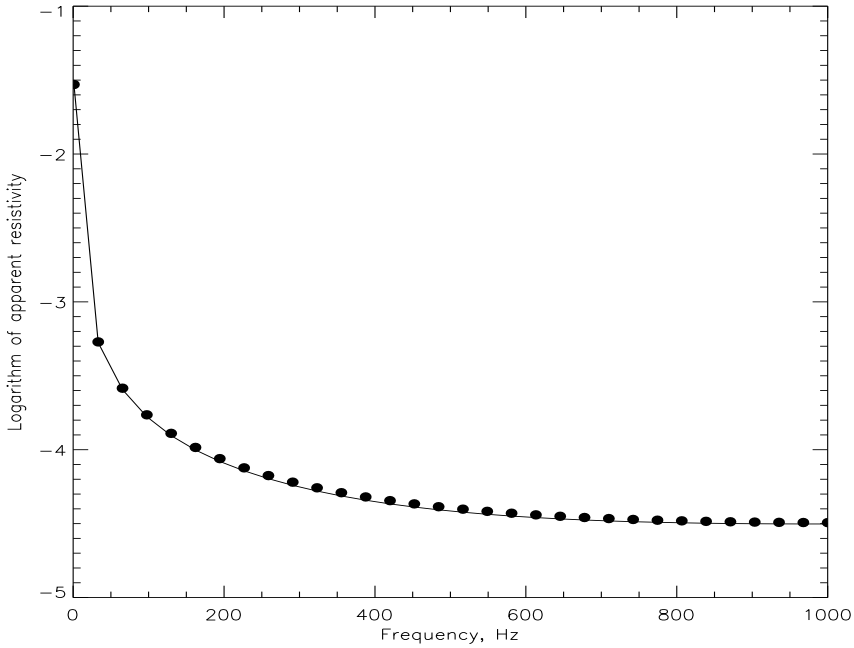

Figure 2: The apparent resistivity for the four layer medium. The analytical solution (solid) in comparison with the numerical solution (filled bullets) for the frequency band [1, 1000] Hz

6.3. Implementation of the sequential minimization procedure. Following the procedure of sequential minimization (see Section 3.3.2), we first discretize the interval $[1, \Omega]$ by using a semi-uniform grid because of the strong filtering effect of seawater. Specifically, we use a uniform grid with sufficiently small step when discretizing the interval $[1, 50]$ and another uniform grid with much larger step when discretizing its complement. As a result, the discrete analogues of complex-valued functions w, w', w'', p, p', p'', a_i, F, Ψ, $\hat{k}_b$ defined on the interval $[1, \Omega]$ for each fixed ξ generate the complex vectors belonging to C^m. For convenience, we shall preserve the same notations for the corresponding vectors, so that the symbol ω denotes below a real vector belonging to the Euclidean space R^m. In addition, we precompute the vectors $\hat{F} = \frac{\hat{\varphi}}{\omega}[\frac{\hat{\varphi}}{\omega} - 2\hat{\varphi}']$ and $\hat{\Psi} = \frac{1}{\omega}[\frac{\hat{k}_b(\omega)+\hat{\varphi}(\omega)}{\omega} - \hat{k'}_b(\omega) - \hat{\varphi}'(\omega)]$. Here, the symbol $'$ means a certain finite-difference approximation of the first derivative of the function $\varphi(\omega)$. To compute $\hat{\varphi}'$, we use Stechkin's regularizator (see, e.g., [28]).

To solve numerically all the $n-1$ minimization problems (37) indicated in Section 3.3.2, the set $\tilde{G}(M)$ needs to be specified. In general, the construction of constraints can be accomplished in several ways. If no *a priori* information about the problem to be solved is available, we take the following nonlinear constraints for each fixed $i = 1, 2, \ldots, n-1$:

$$0 \leqslant \big|a_i(\omega)\big| \leqslant B. \tag{151}$$

Here $a_i = (\Re(a_i), \Im(a_i))$ is the $2m$-dimensional real vector and $B > 0$ is a certain constant. As a result of finite-dimensional approximation, we obtain $n-1$ sets $\mathcal{P}_i$ of constraints. The next stage consists of solving the minimization problems

$$\operatorname{argmin}\big\{ J_{\lambda,i}(a_i) : |a_i| \in \mathcal{P}_i \big\}. \tag{152}$$

In the mathematics literature (see, e.g., [15]), there are available several numerical methods for solving the constrained minimization problems. In our computational experiments, we use the Generalized Reduced

Gradient Method (GRGM) (see, e.g., [15, 29]) because of the nonlinear objective function and constraints. We outline briefly the descent scheme of sequential minimization in algorithmic form

$a_{\text{start}} = \hat{F}$
FOR i=1, n-1 DO BEGIN
Compute a_{3i}
FOR k=1, 2, ... DO BEGIN
$a_i^{(k+1)} = a_i^{(k)} - \beta_k s_k$
IF $|\Delta_k J_{\lambda i}| \leqslant$ **STOP THEN GOTO JUMP**
ENDFOR
JUMP:
$\tilde{a}_i = a_i^{(k_{\text{stop}})}$
Compute $\tilde{\rho}(\tilde{a}_i)$, $\tilde{\eta}_i(\tilde{a}_i)$
$a_{\text{start}} = \tilde{a}_i$
ENDFOR,

where $-s_k$ is the direction of descent. The parameters β_k are chosen so that the relaxation condition, i.e., $J_{\lambda,i}(a_i^{(k+1)}) < J_{\lambda,i}(a_i^{(k)})$, is fulfilled. We accept the kth iteration a_i^k as an approximate minimizer if either the variation $|\Delta_k J_{\lambda,i}|$ between two consecutive iterations of the objective function is less than **STOP** or the Kuhn–Tucker optimality conditions are approximately satisfied to **STOP**. In computational experiments, the number **STOP** is set up 10^{-5}. It should also be pointed out that being a descent method, the GRGM requires the starting vectors to be specified for each subinterval $(\xi_{i-1}, \xi_i]$ $(i = 1, \ldots, n-1)$. The following procedure is adopted for choosing the starting vectors. It follows from (52) – (54) and (72) that the vector $\hat{F}_1$ depending on the data $\hat{\varphi}$ can be taken as a starting vector a_1^{start}. Then, we take consecutively $a_i^{start} = \tilde{a}_{i-1}$ $(i = 2, \ldots, n-1)$. In the sequential minimization algorithm, the starting vectors are determined either from the data $\hat{\varphi}(\omega)$ or from the preceding approximate minimizers $\tilde{a}_i$ $(i = 1, \ldots, n-1)$. Thus, we eliminate the uncertainty in choosing a starting vector inherent in the gradient and Newton-like methods.

The procedure results in the finite set of m-dimensional complex-valued vectors $\{\tilde{a}_i\}_{i=1}^{n-1}$. Given this set, the first derivative of the predicted field $p(\xi, \omega)$ is computed from Eq. (42). Then, the approximate conductivity profile $\tilde{\sigma}(\xi)$ is directly computed from Eqs. (46) – (47). In computational experiments, all integrals are computed using Gaussian quadrature formulas.

6.4. Numerical results We apply the sequential minimization algorithm to the simulated data indicated in Section 6.2. In computational experiments, we use the CWFs (see Eq. (35)) with sufficiently large parameter λ varying from 200 to 500. For such values of λ, the changes in the reconstructed conductivity distribution are small. The CWFs provide sufficiently high values of the convexity parameter ρ and, hence, sufficiently high rate of convergence of the GRGM. For the four-, five-, and ten-layer models, the interval $[0, L]$ is discretized into $n - 1 = 31$ subinterval, whereas it is discretized into $n - 1 = 127$ subintervals for two other models.

6.4.1. Inversion of incomplete data It has been mentioned in Section 3.2 that the "cutting" frequency Ω does not necessarily coincide with the upper bound $\omega_{\max}$ of the frequency band. Due to technological or logistic reasons, the upper bound $\omega_{\max}$ often is much less than the frequency Ω providing a sufficient accuracy of the approximate model (29) – (31). Therefore, we first simulate the incomplete data in the frequency band $[1, 200]$ Hz and apply the sequential minimization algorithm for these incomplete data. Figure 3 shows the result of inversion (asterisks) for $B = 10^{-2}$.

We observe that if no *a priori* information is available, the recovered conductivity profile differs significantly from the "exact" profile. This is due to incomplete data and a relatively large approximation error. Under such conditions, the high resolution of the so-called fine structure of $\sigma(z)$ cannot be expected for any regularizing algorithm including the proposed one. However, it is well known from the theory of ill-posed problems (see, e.g., [14]) that the use of *a priori* information about the specific problem to be solved may improve the accuracy of a regularized solution. Therefore, we focus further on exploiting such information in the sequential minimization algorithm.

6.4.2. Using *a priori* information To improve the accuracy of reconstruction, we use *a priori* information about the problem. Specifically, we employ the concept of a support solution. This concept consists of the following. Since the highly conductive seawater plays the role of a low-pass filter with respect to EM field propagated through the water column, the gradients of $\varphi(\omega)$ corresponding to many realistic distributions of conductivity differ slightly at sufficiently high frequencies, say at frequencies greater than $\omega_{\max}$. Moreover, the

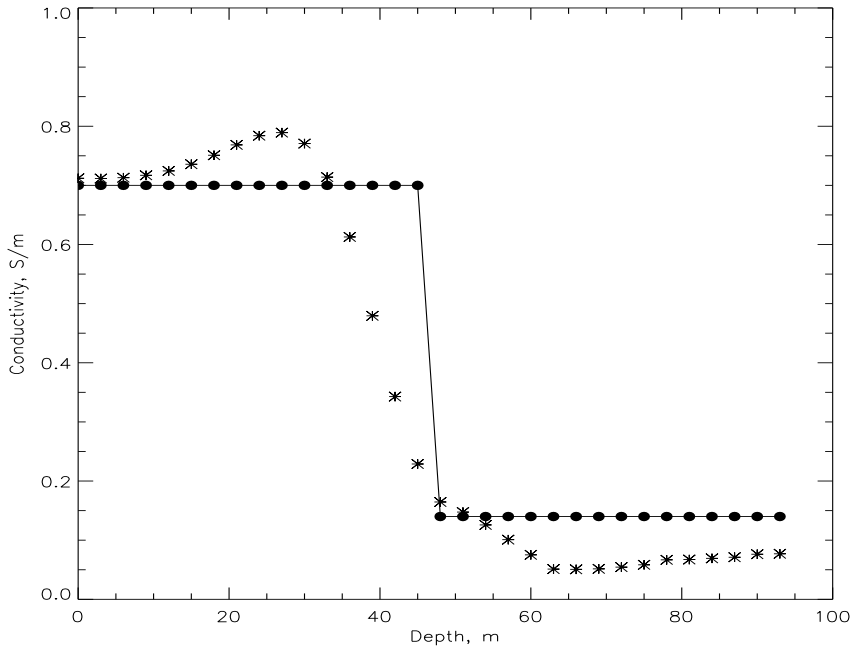

Figure 3: Comparison the "exact" solution (solid) for the four-layer configuration with the conductivity profiles recovered from the incomplete (asterisks) and extended (filled bullets) data

conductivity of seawater σ_w can be estimated from the direct measurements. Therefore, one can introduce the three-layer support model

$$\sigma(z) = \begin{cases} 0 & \text{for} \quad z < 0, \\ \sigma_w & \text{for} \quad 0 \leqslant z < L, \\ \sigma_b & \text{for} \quad z \geqslant L. \end{cases} \tag{153}$$

It should be emphasized that the proximity of this model to the models (138) – (141) is not required when exploiting the sequential minimization algorithm. We can then find the analytical solution to the forward problem (9) – (11) for the support model and use it for extending the sounding data $\varphi(\omega)$, $\omega \in [1, \omega_{\max}]$, on the interval $(\omega_{\max}, \Omega]$. Also, this allows us to decrease significantly the approximation error. As an example, we describe below a simple heuristic procedure for such an extension.

Let $\varphi_3(\omega)$ be the data obtained from this solution. From *a priori* information, the gradients of both the functions $\varphi(\omega)$ and $\varphi_3(\omega)$ are sufficiently close in the interval $\omega \in (\omega_{\max}, \Omega]$. This means that one can extend the data $\varphi(\omega)$ on the interval $(\omega_{\max}, \Omega]$ by adding $\varphi_3(\omega)$, $\omega \in (\omega_{\max}, \Omega]$ and eliminating the jump at $\omega = \omega_{\max}$. Specifically, the extended data are defined as

$$\hat{\varphi}(\omega) = \begin{cases} \varphi(\omega), & [1, \omega_{\max}], \\ \hat{\varphi}_3(\omega), & (\omega_{\max}, \Omega], \end{cases} \tag{154}$$

where

$$\hat{\varphi}_3(\omega) = \begin{cases} \varphi_3(\omega) + \Delta(\omega_{\max}) \text{ if } \varphi(\omega_{\max}) \geqslant \varphi_3(\omega_{\max}), \\ \varphi_3(\omega) - \Delta(\omega_{\max}) \text{ if } \varphi(\omega_{\max}) < \varphi_3(\omega_{\max}) \end{cases} \tag{155}$$

and $\Delta(\omega_{\max}) = \varphi(\omega_{\max}) - \varphi_3(\omega_{\max})$. Figure 4 shows the result of extending the data on the interval (200, 1000] Hz in terms of the logarithmic apparent resistivity for the four-layer model. After extending the data, the level of the total relative error does not exceed 10^{-4} for all the four models indicated above.

Given the three-layer support configuration, we compute consecutively the vectors u_3, p_3, a_{3i} and derive m nonlinear constraints (instead of (151)) for each fixed $i = 1, 2, \ldots, n-1$ for the minimization problems (152). These constraints are as follows:

$$0 \leqslant \left|a_i(\omega)\right| \leqslant \alpha \left|a_{3i}(\omega)\right|,$$

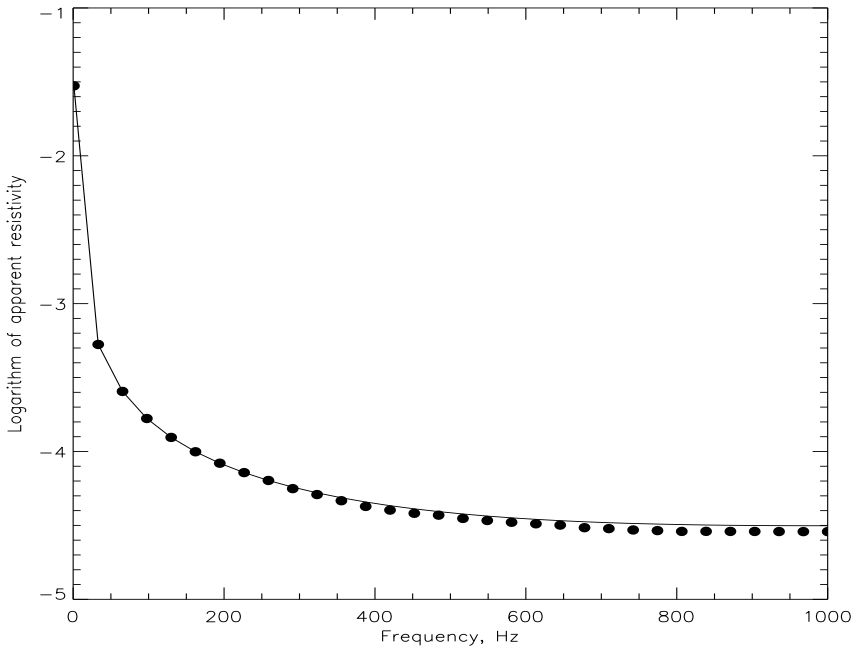

Figure 4: The "exact" data (solid) for the four-layer model in comparison with the extended data (154), (155) for the frequency band [200, 1000] Hz (filled bullets)

where $\alpha > 1$ is a certain number. We have found that the minimizers of the corresponding minimization problems were not significantly changed if $\alpha \in [2, 100]$. In Figure 5, we plot these constraints for the first subinterval, i.e., $i = 1$ for the four-layer model.

The incomplete data simulated in the frequency band $[1, 200]$ Hz have been extended to the band $(200, 1000]$ Hz using the corresponding three-layer support configurations. In addition, we use the constraints derived from the support model. Figures 3 (bullets) and 6 demonstrate the performance of the sequential minimization algorithm for the realistic shallow water sediment configurations. In Figure 3, we see that the accuracy of the recovered conductivity profile can significantly be improved when using *a priori* information in the form indicated above. In Figure 7, we plot the reconstructed profile for the synthetic ten-layer sediment configuration in order to demonstrate the resolution power of the sequential minimization algorithm when using *a priori* information. Finally, Figure 8 shows its performance when identifying the mine modelled as an infinite highly conductive layer.

Thus, we have demonstrated that in the case of "noiseless" data, the use of *a priori* information is crucial for providing the high accuracy of reconstruction. It should also be pointed out that the similar situation takes place when applying the Newton-like methods to 1-D MT (EM) frequency sounding "noiseless" data and using *a priori* information about the interface positions. As an example, we refer to the paper [30] in which the performance of the Levenberg–Marquardt and regularized Newton–Kantorovich methods was numerically studied for the same marine configurations. The results of reconstruction are similar to the results indicated in Figures 3 (filled bullets) and 6 only if the "good" starting vectors were chosen. We also refer to the paper [17] (see Figures 1 and 5 c) demonstrating similar results.

To model the noisy data, we use the simple stochastic model

$$\tilde{\varphi} = \varphi + \sigma\xi, \tag{156}$$

where $\sigma > 0$ is the standard deviation and ξ is the normally distributed pseudo-random vector with a mean of zero and a standard deviation of one. In the computational experiments, we use one hundred samples of the stochastic vector $\tilde{\varphi}$. Figure 9 demonstrates the performance of the proposed algorithm in the case of noisy data. The triangles and diamonds represent the mean values of the conductivity profile reconstructed from the noisy sounding data with the standard deviations 0.0292 and 0.0527. The corresponding levels of noise are five and ten percent, respectively.

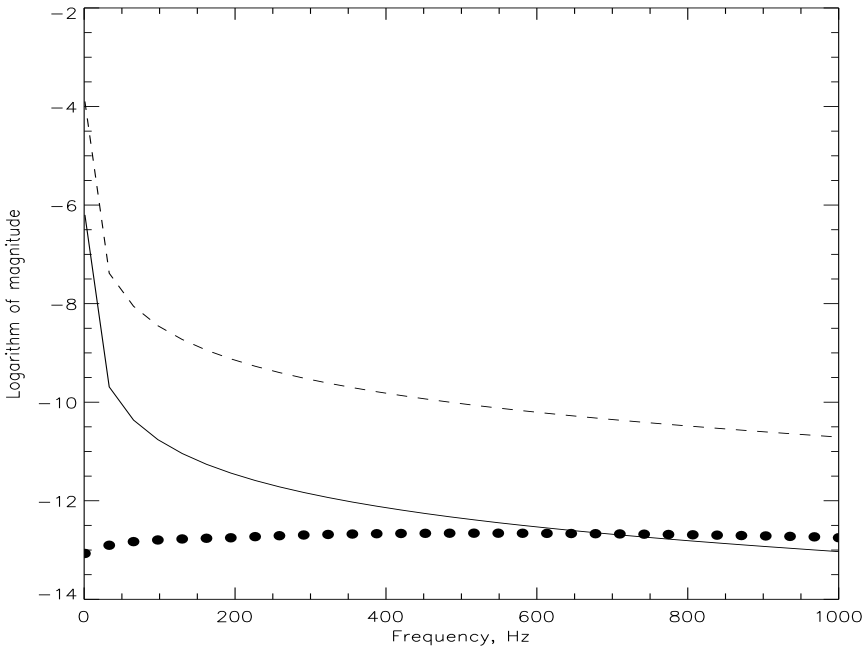

Figure 5: The magnitude of the "exact" coefficient a_1 (solid), constraint (dashed), and starting vector (filled bullets)

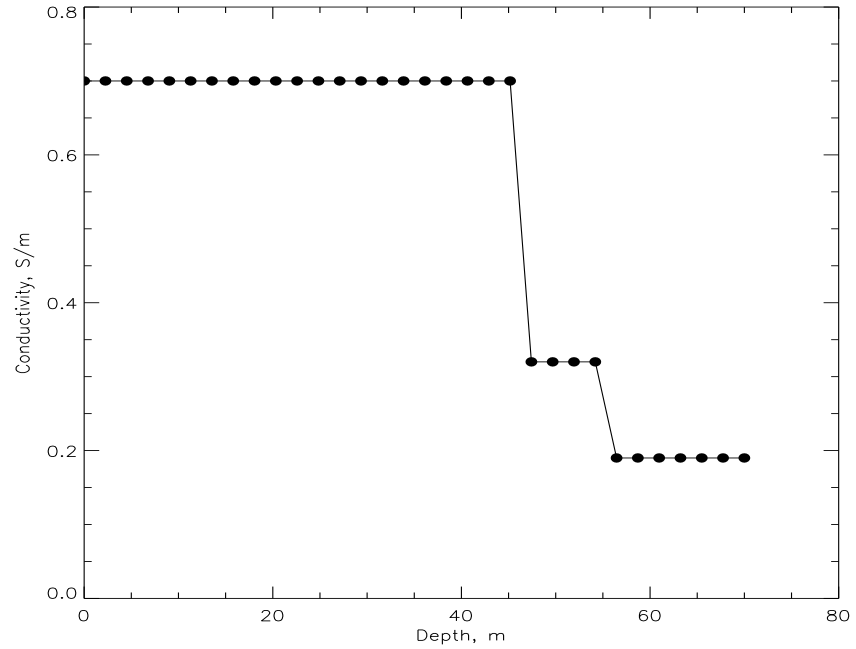

Figure 6: The reconstructed conductivity profile (filled bullets) in comparison with the "exact" solution (solid) for the five-layer configuration

7. Conclusions. We have constructed the sequential minimization algorithm that implements the convexification approach to the 1-D inverse problems of electromagnetic frequency sounding. It can also be applied to solve the inverse problems for more general equation $u'' + [\omega^2\alpha(\xi) + i\omega\beta(\xi) + \gamma(\xi)]u = 0$. Whereas the gradient or Newton-like methods require *a priori* information about the "good" starting vector, the proposed

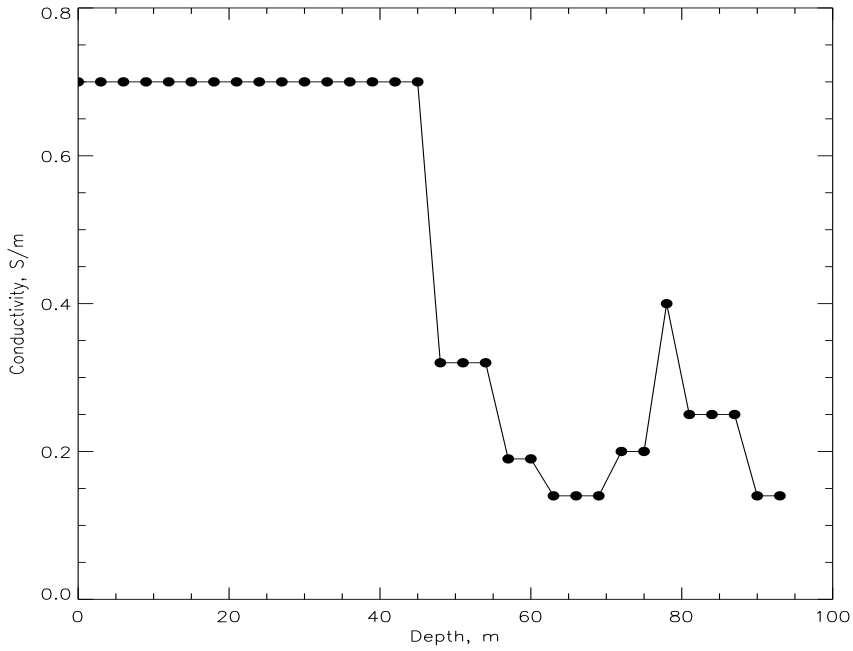

Figure 7: The reconstructed conductivity profile (filled bullets) in comparison with the "exact" solution (solid) for the ten-layer configuration

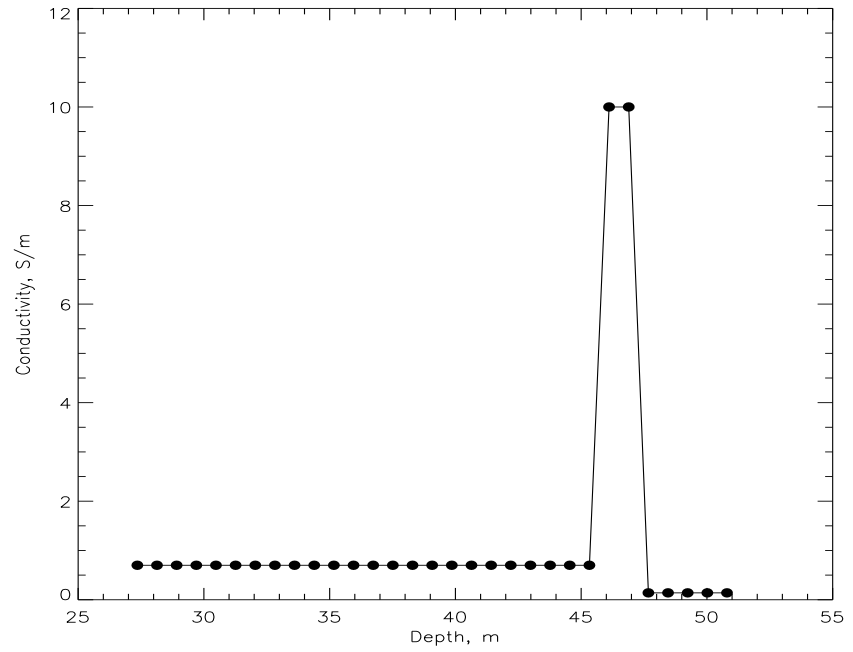

Figure 8: The reconstructed conductivity profile (filled bullets) in comparison with the "exact" solution (solid) for the five-layer configuration containing the modeled mine layer

algorithm utilizes the available sounding data providing the convergence to the approximate solution on the correctness set. A clear physical interpretation can be provided for the procedure of sequential minimization. Indeed, transforming the original inverse problem to an auxiliary one, we reformulate it in terms of prediction of the electromagnetic field from the surface into an inhomogeneous layer. Since the field prediction problem is,

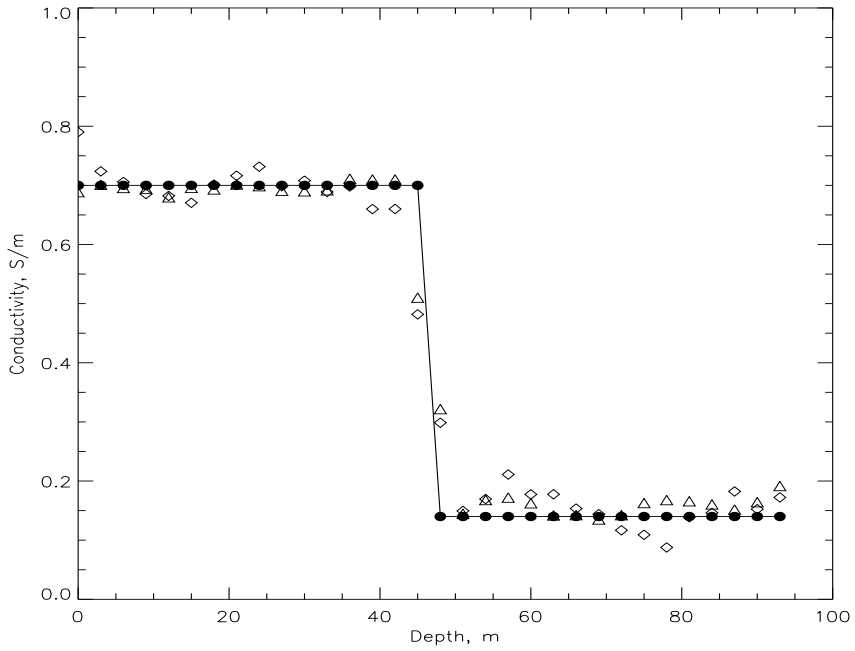

Figure 9: The conductivity profile recovered from the noiseless data (filled bullets) in comparison with the "exact" (solid) and mean values of approximate solutions (triangles and diamonds) for the four-layer configuration

in general, unstable, we construct the layer stripping-like procedure dividing the spatial domain of the unknown conductivity distribution into a finite set of subintervals and approximating the spatial dependence of the field in each subinterval by a quadratic polynomial with frequency-dependent coefficients. Using the Carleman weight functions, we stabilize the field prediction when advancing into the inhomogeneous layer. Once the predicted field is computed, the inversion of sounding data is explicitly performed.

In addition, we indicate here several prospective directions for research. First, to make the sequential minimization algorithm applicable to the real data, we need to test its performance for noisy components of electromagnetic field and improve the algorithm if required. Second, it is our intention to construct some iterative algorithms exploiting the contraction property indicated in Lemma 5. Third, we plan to extend our approach to some inverse problems of acoustic frequency sounding of absorbing media and infrared optical sensing of a human body. We also plan to extend the sequential minimization algorithm to the 2-D and 3-D models making possible a unified framework of the convexification approach applicable to a broad class of multidimensional coefficient inverse problems.

Acknowledgments. We thank Dr. Krylstedt and Dr. Mattsson for supplying one of the authors (AT) with particular marine configurations of the Stockholm archipelago used in computational experiments.

Appendix A

Proof of Lemma 1. Since (6) – (8) is a modification of the Sturm–Liouville problem, its uniqueness implies the existence. Assume that this problem has two different solutions u_1 and u_2. Let $v = u_1 - u_2$; it satisfies the boundary value problem

$$v''(z,\tilde{\omega}) - i\mu\tilde{\omega}\sigma(z)v(z,\tilde{\omega}) = 0, \quad 0 < z < L, \tag{157}$$

$$v(0,\tilde{\omega}) = 0, \tag{158}$$

$$v'(L,\tilde{\omega}) + k_b(\tilde{\omega})v(L,\tilde{\omega}) = 0. \tag{159}$$

Let $\overline{v}$ be the complex conjugate of the function v. Multiplying (157) by $\overline{v}$ and integrating from 0 to L over z, we obtain

$$\int_0^L |v'|^2 dz + i\mu\tilde{\omega}\int_0^L \sigma(z)|v|^2 dz + k_b\left|v(L,\tilde{\omega})\right|^2 = 0.$$

Separating the real and imaginary parts, we obtain

$$\int_0^L |v'|^2 dz + \frac{1}{\sqrt{2}}\sqrt{\mu\tilde{\omega}\sigma_b}\left|v(L,\tilde{\omega})\right|^2 = 0,$$

$$\mu\tilde{\omega}\int_0^L \sigma(z)|v'|^2 dz + \frac{1}{\sqrt{2}}\sqrt{\mu\tilde{\omega}\sigma_b}\left|v(L,\tilde{\omega})\right|^2 = 0.$$

Hence, $v(z,\tilde{\omega}) \equiv 0$.

Now we show that $u(z,\tilde{\omega}) \neq 0$ on $[0,L]\times[\tilde{\omega}_{\min},\infty)$. Assume that the opposite is true, i.e., there exists a pair $(z_0,\tilde{\omega}_0)$ such that $u(z_0,\tilde{\omega}_0)=0$, $(z_0,\tilde{\omega}_0)\in[0,L]\times[\tilde{\omega}_{\min},\infty)$. Because of (7), $z_0\neq 0$. Suppose $z_0\in(0,L)$. It follows from the uniqueness result that $u(z,\tilde{\omega}_0)=0$ for $z\in[z_0,L]$. This implies that $u(z,\tilde{\omega}_0)=0$ for all $z\in[0,L]$, which contradicts to (7). Let $z_0=L$. It follows from (8) that $u'(z_0,\tilde{\omega}_0)=u(z_0,\tilde{\omega}_0)=0$. However, this leads to $u(z,\tilde{\omega}_0)=0$ for all $z\in[0,L]$.

Thus, Lemma 1 is proved.

Appendix B

In this appendix, we discuss the uniqueness results for Inverse Problems I and II. We first point out that the solution $u(z,\tilde{\omega})$ to the boundary value problem (6) – (8) is an analytic function of real variable $\tilde{\omega}$. Hence, the uniqueness result for Inverse Problem II follows from the uniqueness result for Inverse Problem I. Therefore, below we consider Inverse Problem I only. In the case of piecewise analytic function $\sigma(z)$, the uniqueness theorem for this problem was first proven in [3]. If $\sigma(z)\in C^2[0,\infty)$, $\sigma(z)>\text{const}>0$, $\sigma_b>0$, the analogous result can also be established. We outline briefly the proof.

First, we observe that the solution of problem (6) – (8) can be extended on the half-axis $(0,\infty)$ via solving the problem

$$u''(z,\tilde{\omega}) - i\mu\tilde{\omega}\sigma(z)u(z,\tilde{\omega}) = 0, \quad 0<z<\infty, \tag{160}$$

$$u(0,\tilde{\omega}) = 1, \tag{161}$$

$$\lim_{z\to\infty}\left[u'(z,\tilde{\omega}) + k_b(\tilde{\omega})u(z,\omega)\right] = 0. \tag{162}$$

It can be proven that the solutions of boundary value problems (6) – (8) and (160) – (162) coincide for $z\in[0,L)$. Consider an auxiliary hyperbolic boundary value problem

$$\mu\sigma(z)v_{tt} = v_{zz}, \quad 0<z<\infty, \tag{163}$$

$$v(0,t) = \delta(t), \tag{164}$$

$$v(z,0) = v_t(z,0) = 0. \tag{165}$$

We formulate the following problem.

Inverse Problem III. *Given the function*

$$\psi(t) = v_z(0,t), \quad 0<t<\infty, \tag{166}$$

find a function $\sigma(z)$ for which equations (163) – (166) are satisfied.

The following formula holds for a sufficiently large positive $\tilde{\omega}$:

$$u(z,\tilde{\omega}) = \int_0^\infty \exp\left(-\sqrt{i\tilde{\omega}}\,t\right)v(z,t)\,dt. \tag{167}$$

Since (167) is a Laplace-like transform, it is a one-to-one operator. Thus, the uniqueness result for Inverse Problem I follows from the uniqueness result for Inverse Problem III.

Consider the new variable $x=x(z)$ [31]

$$x = \int_0^z \sqrt{\mu\sigma(y)}\,dy \tag{168}$$

and introduce the function

$$S(x) = \sqrt{\frac{\sigma(0)}{\sigma(z(x))}}\,. \tag{169}$$

Let

$$a(x) = \frac{S''(x)}{S(x)} - 2\left[\frac{S'(x)}{S(x)}\right]^2. \tag{170}$$

Then the boundary value problem (163) – (165) can be reduced to the problem

$$v_{tt} = v_{xx} + a(x)v, \quad 0 < x < \infty, \tag{171}$$

$$v(0,t) = \delta(t), \tag{172}$$

$$v(x,0) = v_t(x,0) = 0. \tag{173}$$

The data for this problem are

$$v_x(0,t) = \frac{1}{\sqrt{\mu\sigma(0)}}\,\psi(t). \tag{174}$$

For brevity, we assume that both the values $\sigma(0)$ and $\sigma'(0)$ are known. Then, if the function $a(x)$ is known, then the function $\sigma(z)$ is determined. The uniqueness result for a certain hyperbolic inverse problem, which is similar to problem (171) – (173), was proven in [3] via obtaining the system of Volterra-like integral equations of the second kind. The proof of the uniqueness result for problem (171) – (173) can be analogously obtained. Thus, the following theorem is true.

Theorem 4. *Both the Inverse Problems I and II have at most one solution $\sigma(z)$ satisfying the following conditions:* (1) $\sigma(z) \in C^2[0,\infty)$, (2) $\sigma(z) \geqslant \text{const} > 0$, (3) $\sigma(z) = \sigma_b = \text{const}$ *for* $z > L$, *and* (4) *the values* $\sigma(0)$ *and* $\sigma'(0)$ *are known.*

In addition, it follows from (167) – (173) that the asymptotic behavior of the functions $\partial^s u/\partial z^s(z,\tilde{\omega})$ is

$$\frac{\partial^s}{\partial z^s}\exp\left[-\sqrt{i\tilde{\omega}\mu}\cdot\int_0^z\sqrt{\sigma(y)}\,dy\right]\cdot\left[1+O(\tilde{\omega}^{-1/2})\right], \quad \tilde{\omega}\to\infty, \quad s=0,1,2.$$

This justifies the convergence of the integrals in (17), (132), and (133). In dimensionless variables, the asymptotic formula has the form

$$\sqrt{2\pi}\,\frac{\partial^s}{\partial\xi^s}\exp\left[-\sqrt{i\omega\mu}\cdot\int_0^{L\xi}\sqrt{\sigma(\zeta)}\,d\zeta\right]\cdot\left[1+O(\omega^{-1/2})\right], \quad \omega\to\infty, \quad s=0,1,2.$$

References

1. *Klibanov M.V. and Timonov A.* "A new slant on the inverse problems of electromagnetic frequency sounding: "convexification" of a multiextremal objective function via the Carleman weight functions", *Inverse Problems*, **17**: 1865–1887, 2001.
2. *Tikhonov A.N.* "On determining the electrical characteristics of deep layers of the Earth's crust", *Sov. Math. Dokl.*, 2: 295–297, 1950.
3. *Tikhonov A.N.* "Mathematical basis of the theory of electromagnetic soundings", *U.S.S.R. Comput. Math. Mathemat. Phys.*, **5**: 207–211, 1965.
4. *Cagniard L.* "Basic theory of the magnetotelluric method of geophysical prospecting", *Geophysics*, **37**: 605–635, 1953.
5. *Berdichevsky M.N. and Zhdanov M.S.* Advanced Theory of Deep Geomagnetic Sounding. New York: Elsevier Science Publishing Inc., 1984.
6. *Constable S.C.* "Marine electromagnetic induction studies", *Surv. Geophys.*, **11**: 303–327, 1990.
7. *Palshin N.A.* "Oceanic electromagnetic studies: a review", *Surv. Geophys.*, **17**: 455–491, 1996.
8. MARELEC 96, 99, 01. Proceedings of the 1st, 2nd, and 3rd International Conferences on Marine Electromagnetics. London, UK, June 1997; Brest, France, July 1999; Stockholm, Sweden, July 2001.
9. *Haber E., Asher U.M., and Oldenburg D.* "On optimization techniques for solving nonlinear inverse problems", *Inverse Problems*, **16**: 1263–1280, 2000.
10. *Newman G.A. and Harvesten G.M.* "Solution strategies for two- and three-dimensional electromagnetic inverse problems", *Inverse Problems*, **16**: 1357–1375, 2000.
11. *Dmitriev V.I. and Alekseeva N.V.* "An algorithm for the numerical solution of the inverse problem of MT sounding", in: *Software Library for Geophysics* (in Russian), Moscow: Moscow State University, 1984.
12. *Alexander J.C. and Yorke J.A.* "The homotopy continuation method: numerically implementable topological procedures", *Trans. Am. Math. Soc.*, **242**: 271–284, 1978.

13. *Ramlau R.* "A steepest descent algorithm for the global minimization of the Tikhonov functional", *Inverse Problems*, **18**: 381–403, 2002.
14. *Bakushinsky A.B. and Goncharsky A.V.* Ill-posed Problems: Theory and Applications. Dodrecht: Kluwer Academic Publishers, 1994.
15. *Himmelblau D.M.* Applied Nonlinear Programming. New York: McGraw-Hill, 1972.
16. *Sylvester J.* Layer Stripping. Surveys on Solution Methods for Inverse Problems. Ed. D. Colton, H. Engl, W. Rundell, etc. New York: Springer-Verlag, 2000.
17. *Chen Y., Rokhlin V.* "On the inverse scattering problem for the Helmholtz equation in one dimension", *Inverse Problems*, **8**: 365–391, 1992.
18. *Somersalo E.* "Layer stripping for time-harmonic Maxwell's equations with high frequency", *Inverse Problems*, **10**: 449–466, 1994.
19. *Klibanov M.V. and Timonov A.* "A sequential minimization algorithm based on the convexification approach", *Inverse Problems*, 2003 (to appear).
20. *Levitan B.M.* Inverse Sturm–Liouville Problems. Zeist: VSP, 1987.
21. *Khruslov E.Ya. and Shepelsky D.G.* "Inverse scattering method in electromagnetic sounding theory", *Inverse Problems*, **10**: 1–37, 1994.
22. *Rundell W. and Sacks P.E.* "Reconstruction techniques for classical inverse Sturm–Liouville problems", *Math Comput.*, **58**: 161–183, 1992.
23. *Brown B.M., Samko V.S., Knowles I W., etc.* "Inverse spectral problem for the Sturm–Liouville equation", *Inverse Problems*, **19**: 235–252, 2003.
24. *Isakov V.* Inverse Problems for Partial Differential Equations. New York: Springer, 1998.
25. *Klibanov M.V.* "Global convexity in a three-dimensional inverse acoustic problem", *SIAM J. Math. Anal.*, **28**: 1371–1388, 1997.
26. *Tikhonov A.N.* "On stability of inverse problems", *Sov. Math. Dokl.*, **39**: 195–198, 1943.
27. *Lavrentiev M.M., Romanov V.G., and Shishatskii S.P.* Ill-Posed Problems of Mathematical Physics and Analysis. Providence R.I.: AMS, 1986.
28. *Arestov V.V.* "Approximation of unbounded operators by bounded operators and related extremal problems", *Russian Math. Surv.*, **51**: 1093–1126, 1996.
29. *Lasdon L.S., Waren A.D., Jain A., and Ratner M.* "Design and testing of a Generalized Reduced Gradient Code for nonlinear programming", *ACM Trans. on Math. Software*, **4**: 34–50, 1978.
30. *Krylstedt P., Mattsson J., and Timonov A.* "Numerical modeling of electromagnetic frequency sounding in marine environments: a comparison of local optimization techniques", in: *Proceedings of the 3rd International Conference on Marine Electromagnetics*, Stockholm, Sweden, July 2001.
31. *Romanov V.G.* Inverse Problems of Mathematical Physics. Utrecht: VNU, 1987.

Received 30 January 2003